

An enigmatic new archosauriform from the Carnian–Norian, Upper Triassic, Ischigualasto Formation of northwestern Argentina

IMANOL YÁÑEZ, DIEGO POL, JUAN MARTÍN LEARDI, OSCAR A. ALCOBER,
and RICARDO N. MARTÍNEZ



Yáñez, I., Pol, D., Leardi, J.M., Alcober, O.A., and Martínez, R.N. 2021. An enigmatic new archosauriform from the Carnian–Norian, Upper Triassic, Ischigualasto Formation of northwestern Argentina. *Acta Palaeontologica Polonica* 66 (3): 509–533.

In this contribution we introduce a new Late Triassic archosaur, *Incertovenator longicollum* gen. et sp. nov., with an unusual combination of character states that are present in certain early avemetatarsalian and pseudosuchian archosaur clades. The holotype consists of a partial postcranial skeleton, preserving most of the axial skeleton and displaying a marked anteroposterior elongation in the cervical vertebrae. We include *I. longicollum* gen. et sp. nov. into one of the most comprehensive early archosaur phylogenetic data sets available, and recover it as either an early diverging avemetatarsalian, closely associated with the clade Aphanosauria and Ornithodira, or as an early diverging loricatan closely related to *Mandasuchus tanyauchen* in the most parsimonious trees. We further evaluate which alternative phylogenetic positions can *I. longicollum* gen. et sp. nov. take in the suboptimal trees, and determined which character states support those alternative positions in comparison with those of the unconstrained analysis. The analyses recover the new taxon in three main general phylogenetic placements within Archosauria, as well as one position outside this clade, highlighting widespread morphological evolutionary convergence towards neck elongation in several clades of Triassic archosauriforms.

Key words: Archosauria, Archosauriformes, Ischigualasto, osteology, phylogeny, taxonomy, Triassic, Argentina.

Imanol Yáñez [iyanez@unsj.edu.ar], Instituto y Museo de Ciencias Naturales, Facultad de Ciencias Exactas, Físicas y Naturales, Universidad Nacional de San Juan, Av. España 400 (Norte), San Juan 5400, San Juan, Argentina; and Centro de Investigaciones de la Geósfera y Biósfera, CONICET-UNSJ, Av. Ignacio de la Roza 590, Rivadavia J5400DCS, San Juan, Argentina.

Diego Pol [dpol@mef.org.ar], Museo Paleontológico Egidio Feruglio, CONICET, Av. Fontana 140, Trelew 9100, Chubut, Argentina.

Juan Martín Leardi [jmleardi@gl.fcen.uba.ar], Universidad de Buenos Aires, CONICET, Instituto de Estudios Andinos “Don Pablo Groeber” (IDEAN), Facultad de Ciencias Exactas y Naturales, Departamento de Ciencias Geológicas, Intendente Güiraldes 2160, Ciudad Universitaria, Pabellón 2, Buenos Aires C1428EGBA, Argentina; and Universidad de Buenos Aires, Facultad de Ciencias Exactas y Naturales, Departamento de Biodiversidad y Biología Experimental, Buenos Aires, Argentina.

Oscar A. Alcober [oalcober@unsj.edu.ar] and *Ricardo N. Martínez* [martinez@unsj.edu.ar], Instituto y Museo de Ciencias Naturales, Facultad de Ciencias Exactas, Físicas y Naturales, Universidad Nacional de San Juan, Av. España 400 (Norte), San Juan 5400, San Juan, Argentina.

Received 1 September 2020, accepted 10 December 2020, available online 1 September 2021.

Copyright © 2021 I. Yáñez et al. This is an open-access article distributed under the terms of the Creative Commons Attribution License (for details please see <http://creativecommons.org/licenses/by/4.0/>), which permits unrestricted use, distribution, and reproduction in any medium, provided the original author and source are credited.

Introduction

The rapid and widespread archosauriform radiation resulted in the predominance of these reptiles in terrestrial ecosystems for over 150 million years. Although this radiation started after the Permian–Triassic mass extinction event

(Ezcurra and Butler 2018), it was only by the beginning of the Late Triassic that this group acquired an outstanding ecological diversity and morphological disparity (Foth et al. 2016; Hoffman et al. 2019). One of the most informative faunal assemblages for understanding archosauriform diversity during this transitional time is the Ischigualasto Formation

(Carnian–Norian) of northwestern Argentina (Martínez et al. 2012). The fossil record of the Ischigualasto Formation includes mostly complete specimens of very well-known taxa, but also some key fragmentary specimens (Martínez et al. 2012). Partial specimens are challenging because they can produce unstable branches in phylogenetic analyses due to the missing data and/or character conflict (Kearney and Clark 2003), but they can also be informative and relevant for understanding the relationships of an entire group and assessing instances of homoplasy in several character states (Pol and Escapa 2009).

Here, we describe a new archosauriform from this formation, *Incertovenator longicollum* gen. et sp. nov., that consists of a postcranial skeleton comprising much of a semi-articulated vertebral series, a left ilium, and several other unidentified bone fragments. The new specimen bears an intriguing combination of character states that are plesiomorphic for Archosauria combined with some that are present in early avemetatarsalians (e.g., aphanosaurians) and/or in some pseudosuchian lineages (e.g., early suchians, early crocodylomorphs). The set of features present in the cervical region of *I. longicollum* gen. et sp. nov. suggest that several phylogenetically distant and small-sized archosauriforms convergently acquired elongated necks during the Middle to early Late Triassic evolutionary history of the group.

Institutional abbreviations.—AMNH, American Museum of Natural History, New York, USA; CM, Carnegie Museum of Natural History, Pittsburgh, USA; IVPP, Institute of Vertebrate Paleontology and Paleoanthropology, Beijing, China; NHMUK PV, The Natural History Museum, Palaeontology Vertebrates, London, UK; NMT, National Museum of Tanzania, Dar es Salaam, Tanzania; PVL, Instituto Miguel Lillo, San Miguel de Tucumán, Argentina; PVSJ, División de Paleontología, Museo de Ciencias Naturales de la Universidad Nacional de San Juan, Argentina; TTU-P, Texas Tech University Museum, Lubbock, USA; UCMP, University of Michigan Museum of Paleontology, Ann Arbor, USA; UFRGS, Institute of Geosciences, Federal University of Rio Grande do Sul, Porto Alegre, Brazil.

Other abbreviations.—C, cervical vertebra; Ca, caudal vertebra; D, dorsal vertebra; MPT, most parsimonious trees; S, sacral vertebra.

Nomenclatural acts.—This published work and the nomenclatural acts it contains have been registered in ZooBank: urn:lsid:zoobank.org:pub:D9EA41ED-1810-46AA-B300-E19CB8D93ABA

Geological setting

The Triassic Ischigualasto–Villa Unión sedimentary basin (northwestern Argentina; Fig. 1) is part of a continental rift system that developed during the early Mesozoic along the southwestern margin of Pangea as a consequence of

regional extension processes related to global-scale tectonic phenomena (Ramos and Kay 1991; López-Gamundi et al. 1994; Uliana and Biddle 1988). The infilling of the basin began during the Early Triassic and persisted during the rest of the period (Colombi et al. 2012). The Miocene compressive tectonics related to the uplifting of the Andes generated extensive outcrops of Triassic rocks in homoclinal succession (Milana and Alcober 1994). These outcrops consist of the following stratigraphically ordered units: the Talampaya and Tarjados formations of Early–Middle Triassic; and the Chañares, Los Rastros, Ischigualasto, and Los Colorados formations of Late Triassic age (Milana and Alcober 1994; Rogers et al. 2001; Marsicano et al. 2016). Among these, the Chañares Formation (early Carnian age; Marsicano et al. 2016), the Ischigualasto Formation (Carnian–Norian age; Martínez et al. 2011), and the Los Colorados Formation (middle Norian age; Kent et al. 2014) stand out because of their rich fossiliferous content, particularly among vertebrates (Mancuso et al. 2014; Arcucci et al. 2004).

The thickness of the Ischigualasto Formation ranges from 300 m at the basin margin near the El Alto fault, to more than 700 m at the main depocenter in the El Salto area (Colombi et al. 2012; Fig. 1). The unit is dominated by fluvial and volcanoclastic deposits represented by channel and overbank sandstone, siltstone, and mudstone beds. The depositional environment was characterized as a fluvial system with shallow channels and lakes under a seasonal climatic regime (Rogers et al. 1993; Currie et al. 2009; Colombi et al. 2012). The Ischigualasto Formation can be subdivided into four members from bottom to top: La Peña, Cancha de Bochas, Valle de la Luna, and Quebrada de la Sal (Currie et al. 2009; Fig. 1). These members are distinguished by variations in their sedimentary architecture, paleosol development, and plant taphonomy (Tabor et al. 2006; Colombi 2007; Colombi and Parrish 2008; Currie et al. 2009).

The age of the Ischigualasto Formation is restricted by two $^{40}\text{Ar}/^{39}\text{Ar}$ radioisotopic datings performed at the Ischigualasto Provincial Park (San Juan Province) where the thickness of the formation is approximately 700 m (Martínez et al. 2011). The oldest age (231.4 ± 0.3 Myr) comes from a level of 20 m above of the base of the unit (Rogers et al. 1993), whereas the younger age (225.9 ± 0.9 Myr) comes from a level of 630 m above the base of the unit (Martínez et al. 2011; Fig. 1). Given this evidence, the Ischigualasto Formation spans for approximately 6 Myr, from the late Carnian to the early Norian (Martínez et al. 2011).

Vertebrate assemblage: The vertebrate fauna of the Ischigualasto Formation includes one of the oldest dinosaur assemblages known to date (Bonaparte 1982; Rogers et al. 1993; Brusatte et al. 2010; Martínez et al. 2012), non-archosauriform archosauromorphs, pseudosuchians, synapsids, and temnospondyls. The rhynchosaur *Hyperodapedon* is the most abundant taxon of this fauna, representing nearly 60% of all the recovered specimens (Martínez et al. 2012). The dinosaurian and pseudosuchian components of this fauna are taxonomically diverse but less abundant. Regarding

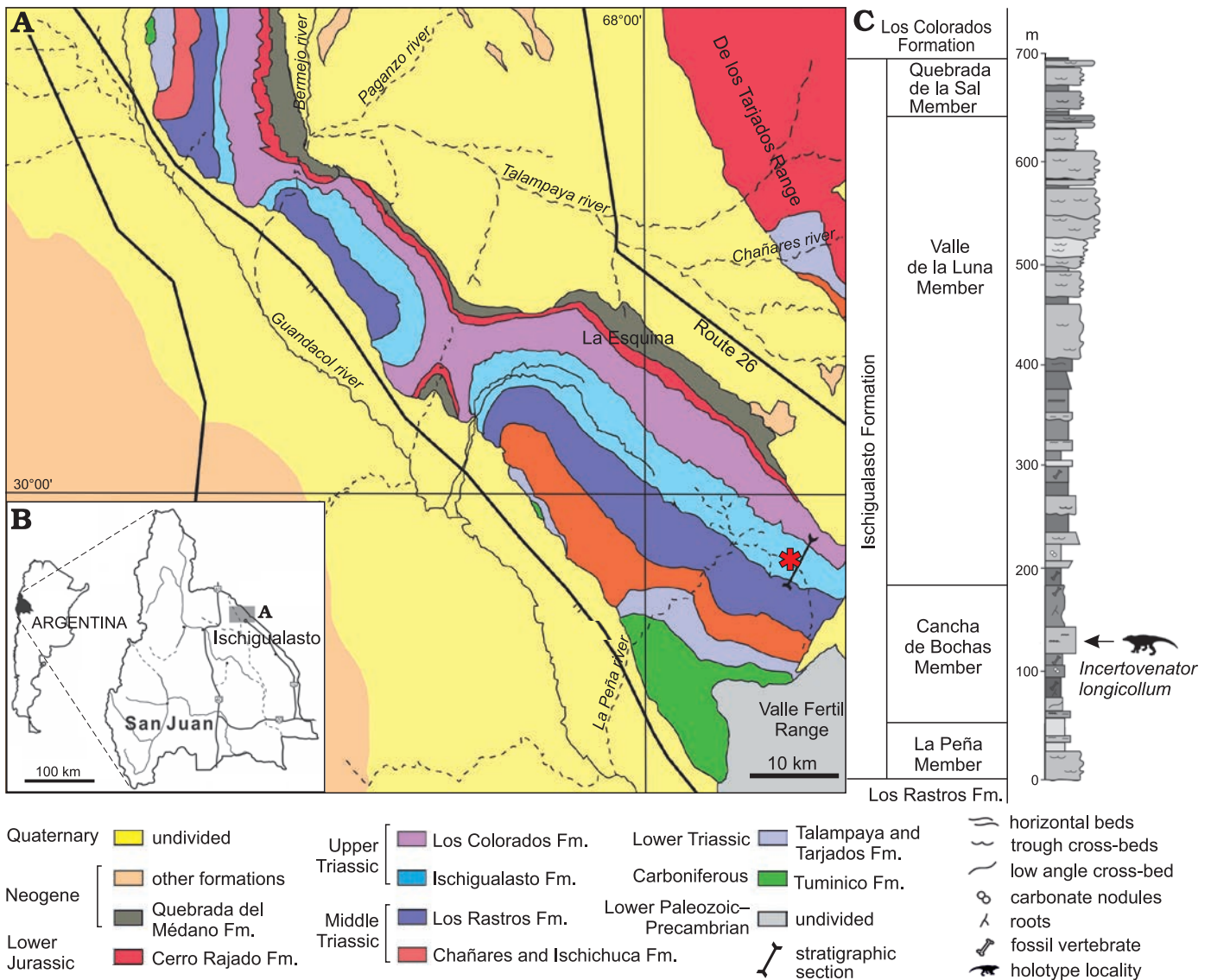


Fig. 1. Geographic and stratigraphic position of the holotype specimen of *Incertovenator longicollum* gen. et sp. nov. (PVSJ 397). **A, B.** Geological map of the Ischigualasto–Villa Unión Basin. Asterisk indicates the type locality. **C.** Stratigraphic section of the Ischigualasto Formation. Modified from Martínez 1994.

pseudosuchians in particular, several species have been described: the aetosaur *Aetosauroides scagliai* (Casamiquela 1960; Desojo 2005; Desojo and Ezcurra 2011), the loricatan *Saurosuchus galilei* (Sill 1974; Alcober 2000; Trotteyn et al. 2011), the poposauroid *Sillosuchus longicervix* (Alcober and Parrish 1997), the ornithosuchid *Venaticosuchus rusconii* (Bonaparte 1970; Baczko et al. 2014), and the crocodylomorph *Trialestes romeri* (Reig 1963; Bonaparte 1978; Lecuona et al. 2016). In this sense, both *Sillosuchus longicervix* and *Trialestes romeri* are the only representative taxa of the clades Poposauroidea and Crocodylomorpha (however, see Leardi et al. 2020), respectively, found to date in the Ischigualasto. Formation *Sillosuchus longicervix* was described based on an incomplete and poorly preserved postcranial skeleton by Alcober and Parrish (1997) and represents the only South American poposauroid known to date. This taxon is diagnosed by the presence of elongated

cervical vertebrae, possibly pneumatic recesses on the lateral sides of cervical and dorsal vertebrae, and relatively short ischia (Alcober and Parrish 1997).

On the other hand, *Trialestes romeri* represents one of the oldest members of Crocodylomorpha known so far (Irmis et al. 2013; Lecuona et al. 2016). The taxonomic identity of *Trialestes romeri* has historically been controversial due in part to the incompleteness of the holotype (PVL 2561) and the poor preservation of the referred material (PVL 3889). In the same way, the presence of an unusual combination of character states has resulted in different interpretations of the taxonomic identity of these materials as well as the phylogenetic placement of *Trialestes romeri* (Reig 1963; Bonaparte 1978, 1982; Benton and Clark 1988; Clark et al. 2001). However, Lecuona et al. (2016) recently redescribed all material assigned to the hypodigm of *Trialestes romeri* and tested its phylogenetic affinities. This study supported

the referral of PVL 3889 to *Trialestes romeri* and recovered this species well nested within non-crocodyliform Crocodylomorpha. On the other hand, Leardi et al. (2017) included the holotype specimen of *Trialestes romeri* (PVL 2561) into their phylogenetic analysis and recovered it in a more basal position within Crocodylomorpha, in comparison to that of Lecuona et al. (2016). The holotype specimen of *Trialestes romeri* and *Pseudhesperosuchus jachaleri* were found forming a South American clade of non-crocodyliform crocodylomorphs restricted to the Late Triassic (Leardi et al. 2017).

Systematic palaeontology

Diapsida Osborn, 1903 (sensu Laurin 1991)

Sauria Gauthier, 1984 (sensu Gauthier et al. 1988)

Archosauriformes Gauthier, Kluge, and Rowe, 1988

?Archosauria Cope, 1869 (sensu Gauthier and Padian 1985)

Genus *Incertovenator* nov.

ZooBank LSID: urn:lsid:zoobank.org:act:8DA8086B-7917-4843-9445-5C901C0212E2

Type species: *Incertovenator longicollum* gen. et sp. nov., monotypic, see below.

Etymology: From the Latin *incerto*, uncertain, and *venator*, hunter; in reference to its uncertain phylogenetic affinities and possible predatory habits.

Diagnosis.—Same as for the type species.

Incertovenator longicollum sp. nov.

Figs. 2–9.

ZooBank LSID: urn:lsid:zoobank.org:act:4B06A555-50E3-4D20-A0A3-031650974E2D

Etymology: From the Latin *longus*, long, and *collum*, neck; referring to its elongated cervical vertebrae.

Holotype: PVSJ 397, incomplete partially articulated postcranial skeleton, including an almost complete axis articulated with the third cervical vertebra, third cervical vertebra nearly complete and articulated with its corresponding complete left rib, one isolated anterior cervical vertebra, two incomplete partially articulated anterior cervical vertebrae, ten articulated mid to posterior dorsal vertebrae, two sacral vertebrae in articulation with the first five caudal vertebrae, an additional caudal centrum fragment attached to the posterior end of the last caudal, almost complete left ilium, and two unidentified bone fragments.

Type locality: Southern outcrops of the Ischigualasto Formation at the Hoyada de Ischigualasto locality (Ischigualasto Provincial Park, San Juan Province, NW Argentina).

Type horizon: The middle levels of the Cancha de Bochas Member (sensu Currie et al. 2009), approximately 120 m above the base of the formation (Fig. 1), and corresponds to the *Scaphonyx–Exaeretodon–Herreriasaurus* Biozone (Martínez et al. 2011, 2012).

Material.—Type material only.

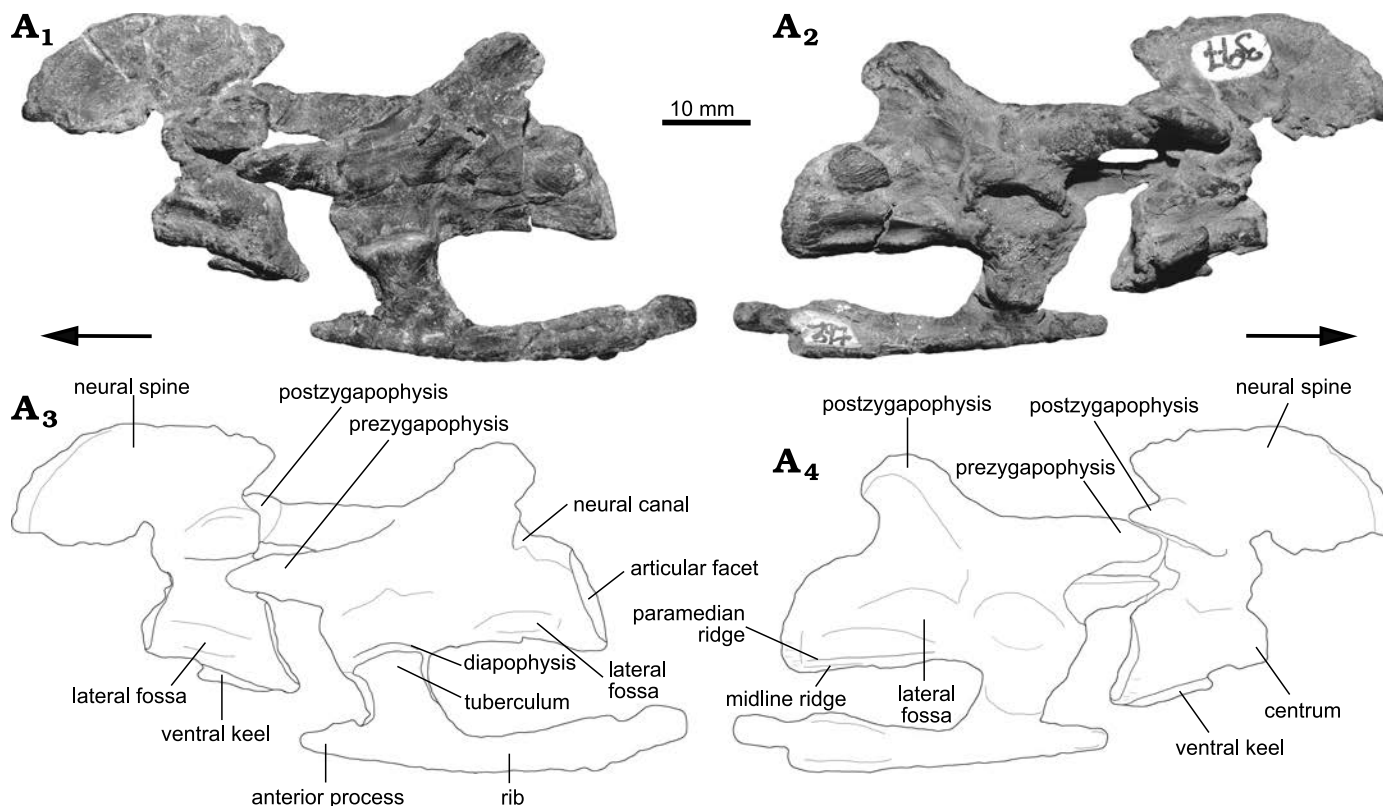


Fig. 2. Photographs (A₁, A₂) and interpretative drawings (A₃, A₄) of the axis, third cervical vertebra and third cervical rib of the archosauriform *Incertovenator longicollum* gen. et sp. nov. (PVSJ 397) from Ischigualasto Formation (Carnian–Norian), Hoyada de Ischigualasto, Argentina; in left (A₁, A₃) and right (A₂, A₄) lateral views. Arrows indicate anterior direction.

Diagnosis.—*Incertovenator longicollum* gen. et sp. nov. differs from all other archosaurs in the possession of the following unique combination of characters states: anterior cervical vertebrae with a centrum length 2.5 times longer than high; axial neural spine with a dorsally convex margin; anterior cervical vertebrae neural spines anteroposteriorly longer than high; anterior cervical neural spines with anterior overhang; anterior cervical neural spines with a rugose expansion at its distal end; dorsal vertebrae neural spines distal expansions with rounded dorsal margins; dorsal vertebrae neural spines with a posterodorsal tip overhanging the neural arch; ilium with a concave dorsal margin in lateral view; ilium with a long preacetabular process that exceeds the anterior margin of the acetabulum; medially expanded shelf on the postacetabular process that originates at the dorsoventral midpoint of the postacetabular process; ischiadic peduncle of the ilium vertically oriented in lateral view; ventral margin of the ilium with convex (closed) acetabulum.

Description.—*Axial skeleton:* The axial skeleton is relatively well represented and includes vertebral centra, neural arches, neural spines, and ribs. However, the dorsoventral deformation of the specimen has produced a displacement relative to the sagittal plane of parts of the neural arch, like articular the surfaces with the ribs, neural arch pedicels, and zygapophyses. Additionally, some vertebrae are fractured, and some of their components were found disarticulated (e.g., centra and their respective neural arches), though closely associated. Vertebrae from all regions of the axial skeleton are preserved. Overall, all vertebral centra are anteroposteriorly longer than dorsoventrally high (measured to the top of the articular facets) and dorsoventrally higher than lateromedially wide (see Tables 1–3). All vertebral centra have longitudinally concave and dorsoventrally convex lateral surfaces. This “spool-shaped” morphology

is a condition widely distributed within Archosauria, as seen in avemetatarsalians like *Teleocrater rhadinus* (Nesbitt et al. 2018), *Silesaurus opolensis* (Dzik 2003), *Lewisuchus admixtus* (Romer 1972; Bittencourt et al. 2015), *Eoraptor lunensis* (Serenó et al. 1993, 2012) and *Eodromeus murphi* (Martínez et al. 2011), among others; as well as in pseudosuchians like *Gracilisuchus stipanicorum* (Lecuona et al. 2017), *Ticinosuchus ferox* (Krebs 1965; Lautenschlager and Desojo 2011), *Xilousuchus sapingensis* (Nesbitt et al. 2010a), *Sillosuchus longicervix* (Alcober and Parrish 1997) and *Trialestes romeri* (Lecuona et al. 2016), among others.

Cervical vertebrae: The preserved cervical vertebrae (C) include a nearly complete axis articulated with an almost complete third cervical vertebra, an isolated complete anterior cervical vertebra and two incomplete and partially articulated anterior cervical vertebrae (Figs. 2–4). As the latter three vertebrae are not articulated with the third cervical vertebra, their placement within the cervical series was interpreted based on the relative position of the parapophyses and diapophyses on the centra and neural arches, respectively, and compared to other well-known archosaurs that preserve some of all of the cervical region (see below). In the isolated cervical vertebra, the parapophyses are placed on the anteroventral margin of the centrum while the diapophyses are placed on the anteroventral margin of the neural arch, bordering the anterior articular facet of the centrum, as indicated by the position of the capitulum and tuberculum of the rib, respectively (Fig. 3). Of the other two incomplete and partially articulated cervical vertebrae, only the posterior-most vertebra preserves its corresponding parapophyses and diapophyses. These structures are also located on the anteroventral margin of the centrum and neural arch, respectively (Fig. 4). The relatively anterior and ventral location of the parapophyses and diapophyses

Table 1. Selected measurements (in mm) of the cervical vertebrae (C3–C6) of *Incertovenator longicollum* (PVSJ 397). All measurements are the maximum measurable. [] estimated measurement; * incomplete element; || an element (e.g., a vertebral centrum) that is not completely preserved (e.g., in anteroposterior length) but was measured nonetheless.

| | | Axis | C3 | C4 | C5 | C6 |
|----------------------------------|--------|-----------------|-----------------|-----------------|-------|--------|
| Centrum length | | 20.7* | 36.0* [40.0] | 35.7* [37.0] | 17.4* | 28.8* |
| Centrum length/height ratio | | 1.66* | 2.69* [2.98] | 2.88* [2.98] | 1.28* | 2.01* |
| Maximum height | | 31.2 | 20.1* | 33.5 | – | – |
| Anterior articular facet | height | – | – | 12.4 | – | 14.3 |
| | width | – | – | 10.0 | – | 12.2 |
| Posterior articular facet | height | 12.5 | 13.4 | – | 13.6 | – |
| | width | 10.6 | 11.7 | 7.4* [10.6] | 11.4 | – |
| Neural arch length | | 10.3* [30.6] | 26.9 | 35.3 | – | – |
| Neural spine | length | 31.6 | – | 27.0 | 22.4* | 19.2 |
| | height | 17.0 | – | 11.2 | 13.0 | [10.6] |
| Neural spine length/height ratio | | 1.86 | – | 2.41 | 1.72* | 1.81 |
| Prezygapophyses length | | – | 18.9 | 19.0 | – | 17.9 |
| Postzygapophyses length | | 13.1 | – | 21.0 | 22.3 | – |
| Anterior neural canal | height | – | 6.3 | 4.7 | – | – |
| | width | – | 4.6 | 3.3 | – | – |
| Posterior neural canal | height | [5.2] | 6.9 | – | – | – |
| | width | [2.2] | 4.5 | – | – | – |

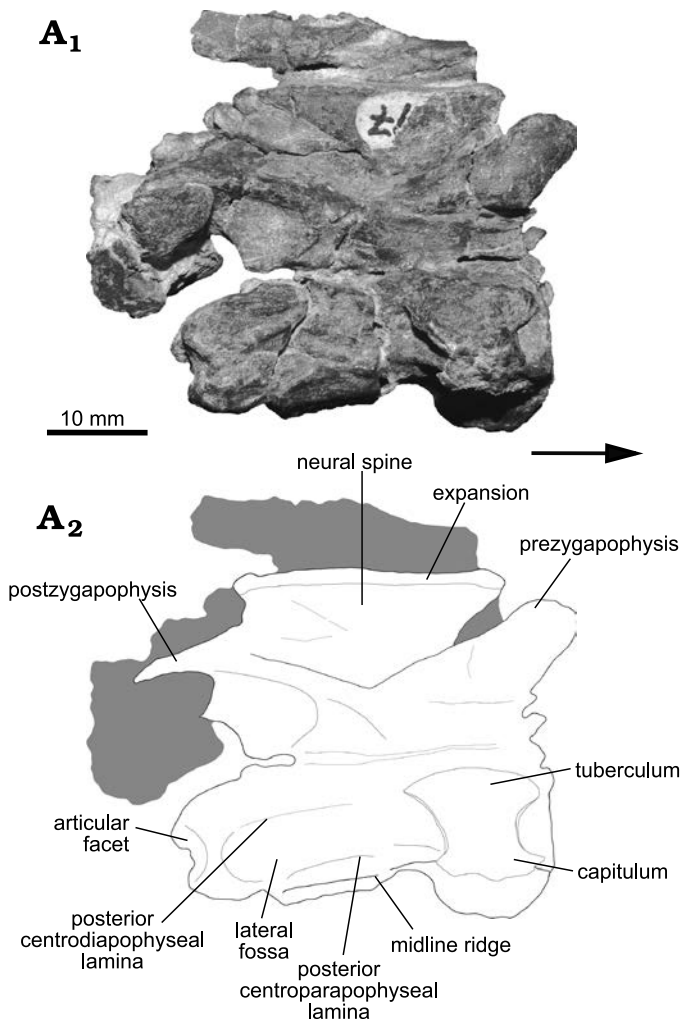


Fig. 3. Photograph (A₁) and interpretative drawing (A₂) of isolated anterior cervical vertebra of the archosauriform *Incertovenator longicollum* gen. et sp. nov. (PVSJ 397) from Ischigualasto Formation (Carnian–Norian), Hoyada de Ischigualasto, Argentina; in right lateral view. Grey coloring represents broken bones and other fragments. Arrow indicates anterior direction.

for the latter three vertebrae suggests that these vertebrae most likely correspond to the anterior-to-middle portion of the cervical region (C1–C6). A similar cervical morphology is frequent within Archosauria and can be observed in taxa such as *Teleocrater rhadinus* (Nesbitt et al. 2018), *Yarasuchus deccanensis* (Sen 2005), *Spondylosoma absconditum* (Huene 1942; Galton 2000), *Silesaurus opolensis* (Dzik 2003), *Xilousuchus sapingensis*, IVPP V 6026, (Wu 1981; JML personal observation) *Hesperosuchus agilis*, AMNH 6758, (Colbert 1952), *Dibothrosuchus elaphros* (Wu and Chatterjee 1993) and *Terrestriusuchus gracilis* (Crush 1984). Nevertheless, the exact topological location of the three posteriormost anterior-to-middle cervical vertebrae of *Incertovenator longicollum* gen. et sp. nov. cannot be confidently determined because there is no discernible difference in the position of either the parapophyses or the diapophyses between two of these vertebrae (Figs. 3, 4).

The axis is well preserved and only lacks the odontoid process and the anterior half of the vertebral centrum and

neural arch (Fig. 2). The centrum is dorsoventrally higher than mediolaterally broad and, although the vertebra lacks the anterior half of the centrum and neural arch, the anteroposterior extent of the neural spine and its well developed ventral base for articulation with the neural arch suggest that the centrum is anteroposteriorly longer than dorsoventrally tall. This axial morphology is widely spread across Archosauria but contrasts with most non-crocodylomorph loricateans where the axial centrum is dorsoventrally higher than anteroposteriorly long (e.g., *Saurosuchus galilei*, Trotteyn et al. 2011; *Batrachotomus kupferzellensis*, Gower and Schoch 2009; *Fasolasuchus tenax*, Bonaparte 1981; *Postosuchus kirkpatricki*, TTU-P 9235, Weinbaum 2013), with the notable exceptions of *Mandasuchus tanyauchen* (Butler et al. 2018) and *Polonosuchus silesiacus* (Sulej 2005). The ventral surface of the centrum bears a well-developed midline keel that runs along the preserved length of the centrum (Fig. 2A₃, A₄), a condition also observed in avemetatarsalians, such as *Teleocrater rhadinus* (Nesbitt et al. 2018), *Yarasuchus deccanensis* (Sen 2005), *Lewisuchus admixtus* (Bittencourt et al. 2015) and *Silesaurus opolensis* (Dzik 2003), but also in other pseudosuchians as *Gracilisuchus stipanicorum* (Lecuona et al. 2017), *Arizonasaurus babbitti* (Nesbitt 2005), *Xilousuchus sapingensis* (Nesbitt et al. 2010a), *Mandasuchus tanyauchen* (Butler et al. 2018), *Dibothrosuchus elaphros* (Wu and Chatterjee 1993) and *Pseudhesperosuchus jachaleri* (Bonaparte 1971). A distinct shallow fossa is located on the lateral surface of the centrum, just ventral to the inferred position of the neurocentral suture. This fossa is dorsally and ventrally bounded by two low ridges that are parallel at mid-centrum length but slightly diverge posteriorly where they reach the border of the posterior articular facet (Fig. 2A₁, A₃). Similar shallow fossae are present on the axial centrum of *Teleocrater rhadinus* (Nesbitt et al. 2018), *Lewisuchus admixtus* (Bittencourt et al. 2015), *Silesaurus opolensis* (Dzik 2003), *Arizonasaurus babbitti* (Nesbitt 2005), *Dibothrosuchus elaphros* (Wu and Chatterjee 1993) and *Pseudhesperosuchus jachaleri* (Bonaparte 1971). The absence of the anterior half of the centrum precludes determining the point of origin of these ridges. The posterior articular facet of the axial centrum is anterodorsally slanted in lateral view (Fig. 2) and slightly lateromedially compressed, having an oval shape.

The posterior neural arch pedicels of the axis are as high as the centrum and they extend posteriorly contacting the border of the posterior articular facet. The neural canal is small in diameter and elliptical in shape, with the dorsoventral axis longer than the mediolateral axis. The postzygapophyses are long, extending posteriorly as far as the margin of the posterior articular facet. The postzygapophyseal articular facets are ventrolaterally directed, forming an angle of approximately 30° with the horizontal. There is no evidence of epipophyses. The axial neural spine is anteroposteriorly long and is as dorsoventrally high as the centrum (Table 1). The neural spine extends posteriorly as far as the level of the postzygapophyses. In lateral view, the dorsal margin of

neural spine is dorsally convex and slopes anteroventrally forming an arch that ends at the same dorsoventral level as the base of the postzygapophyses (Fig. 2). The posterior margin of the axial neural spine is directed posterodorsally forming an acute angle with the dorsal margin. This morphology is strikingly similar to the axial neural spine of *Lewisuchus admixtus* (Bittencourt et al. 2015), where the anterior height of the neural spine is nearly equivalent to the posterior height. It also resembles the axial neural spines of the pseudosuchians *Erpetosuchus granti* (Benton and Walker 2002), *Ticinosuchus ferox* (Krebs 1965), and *Mandasuchus tanyauchen* (Butler et al. 2018). Among avemetatarsalians, the presence of a neural spine with a convex dorsal margin is present in *Silesaurus opolensis* (Dzik 2003), and in *Marasuchus lilloensis* (PVL 3870) and *Coelophysis bauri*, as reported by Nesbitt (2011). In ventral view, the anterior half of the base of the axial neural spine of *I. longicollum* gen. et sp. nov. is expanded mediolaterally.

The third cervical vertebra only lacks the neural spine and the distal portion of the postzygapophyses. The vertebra is in articulation with its left cervical rib (see description below) and with the axis (Fig. 2). The anterior portion of the vertebral centrum is poorly preserved, lacking the anterior articular facet. Moreover, the entire neural arch is anteroventrally displaced by post mortem crushing. In ventral view, the centrum bears two low paramedian ridges, but these are only distinguishable along the posterior half of the centrum. Between these ridges there is a faint and less developed midline crest. The presence of paramedian ridges or secondary posterior ventral keels on the cervical vertebrae is reported for *Teleocrater rhadinus* (Nesbitt et al. 2018), *Yarasuchus deccanensis* (Sen 2005) and in some cervicals of *Arizonasaurus babbitti* (Nesbitt 2005). As in the axial centrum, there is a distinct shallow fossa ventral to the inferred position of the neurocentral suture that is bounded by two low ridges (Fig. 2A₂, A₄). These ridges originate at the base of the parapophysis and diapophysis, respectively, and run from the anteroposterior midpoint of the centrum to the posterior articular rim. Based on their origin they can be interpreted as incipiently developed posterior centrodiaepophyseal and posterior centroparapophyseal laminae (sensu Wilson 1999). A similar development of these ridges is present in avemetatarsalians (e.g., *Teleocrater rhadinus*, Nesbitt et al. 2018; *Yarasuchus deccanensis*, Sen 2005; *Asilisaurus kongwe*, Nesbitt et al. 2010b; *Silesaurus opolensis*, Dzik 2003; *Lewisuchus admixtus*, Bittencourt et al. 2015) and in pseudosuchians (e.g., *Gracilisuchus stipanicorum*, Lecuona et al. 2017; *Arizonasaurus babbitti*, Nesbitt 2005; *Xilousuchus sapingensis*, Nesbitt et al. 2010a; *Mandasuchus tanyauchen*, Butler et al. 2018; holotype of *Hesperosuchus agilis*, Colbert 1952, and the crocodylomorph UCMP 12947, Parrish 1993). Due to crushing and displacement of the neural arch, the left parapophysis and diapophysis are artificially placed on a more ventral position on the anterior half of the vertebral centrum and they are covered by the articular heads of the rib (Fig. 2A₁, A₃), preventing further description of these struc-

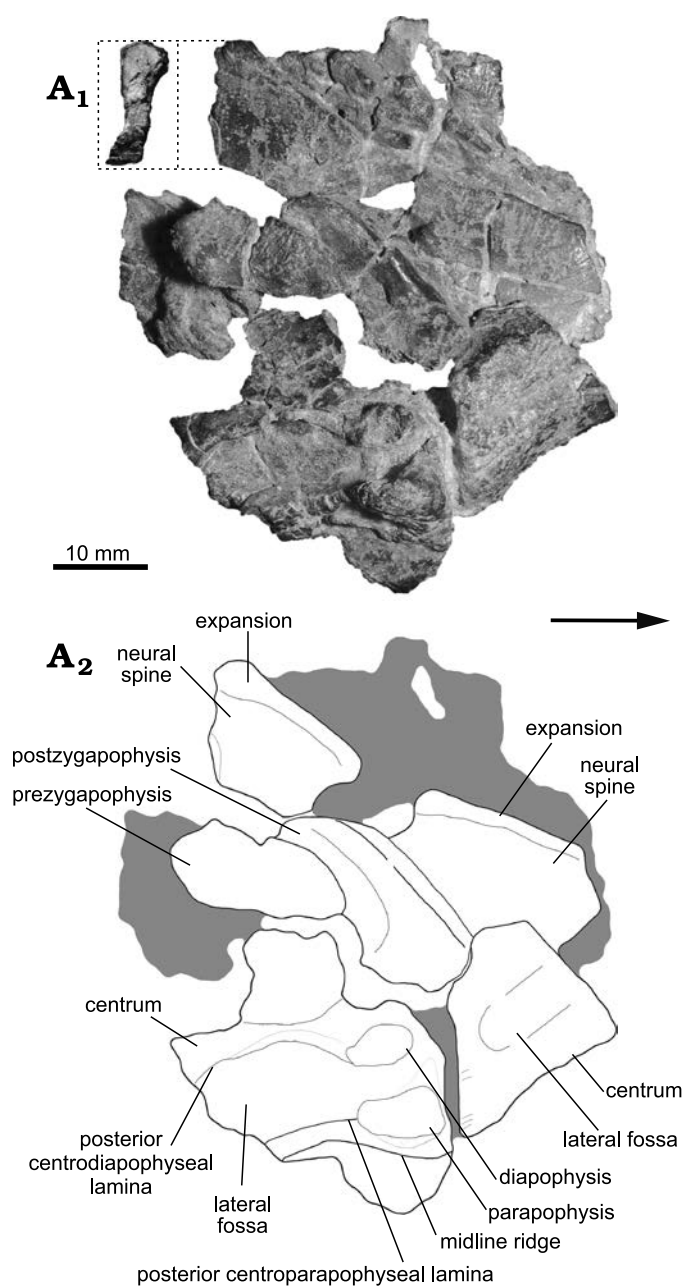


Fig. 4. Photograph (A₁) and interpretative drawing (A₂) of articulated pair of anterior cervical vertebrae of the archosauriform *Incertovenator longicollum* gen. et sp. nov. (PVSJ 397) from Ischigualasto Formation (Carnian–Norian), Hoyada de Ischigualasto, Argentina; in right lateral view. Posterior view of neural spine detailed in inset (stippled lines). Grey coloring represents broken bones and other fragments. Arrow indicates anterior direction.

tures. The right parapophysis and diapophysis are poorly preserved and shifted to a more dorsal position as a result of the deformation mentioned above. The posterior central articular facet is anterodorsally slanted in lateral view and slightly compressed lateromedially, possessing an oval outline in posterior view.

The anteroventral displacement of the neural arch precludes an adequate preservation of its pedicels. In posterior view, the neural canal is elliptical, with the dorsoventral axis longer than the mediolateral axis. The prezygapophyses are

relatively long, approximately half of the centrum length, and are horizontally and anteriorly projected, markedly exceeding the anterior margin of the centrum to contact the axial postzygapophyses (Fig. 2). The prezygapophyseal articular facets are broad and dorsomedially oriented at an angle of approximately 45° with the horizontal. The bases of the postzygapophyses are subtriangular, relatively long, and horizontally projected posteriorly. Their posterior extension cannot be determined because the distal portions are not preserved.

The isolated cervical vertebra is almost complete, only missing the distal portion of the left prezygapophysis and the posterior articular facet, although a portion of the right-lateral border of the posterior articular facet is still visible (Fig. 3). The preservation of its left lateral side is poor because the vertebra is crushed and several rib fragments cover part of the neural arch and spine. As in the third cervical vertebra, the centrum is anteroposteriorly elongated, being almost three times longer than high (Table 1). The centrum is mediolaterally compressed and bears a well-developed midline ridge on its ventral surface (Fig. 3). As mentioned before, the parapophyses and diapophyses are placed on the anteroventral side of the centrum and neural arch, respectively. These structures are articulated with the corresponding tuberculum and capitulum of the rib, delimiting a vertebrocostal canal. The anterior placement of the parapophyses and diapophyses suggests that the vertebra belongs to the anterior-to-middle region of the cervical series (C1–C6). As in the previous vertebrae, the vertebral centrum has a shallow fossa on its lateral surface delimited by the two low posterior centrodiapophyseal and posterior centroparapophyseal laminae (Fig. 3A₂). These ridges run posteriorly and contact the border of the posterior articular facet. The anterior articular facet is vertically oriented, is subequal in height and width and has a subcircular outline.

The neural arch of the isolated vertebra is mostly disarticulated from the centrum, but remains closely associated. As mentioned before, this separation is interpreted as a consequence of post-depositional crushing rather than an open neurocentral suture, because in the axis and the third cervical vertebra this suture is closed. The neural arch pedicels are dorsoventrally low and anteroposteriorly long, contacting the rim of both anterior and posterior central articular facets. The prezygapophyses are approximately half the length of the centrum, they project anterodorsally, are subparallel to each other, and exceed the anterior centrum margin. The prezygapophyseal articular facets are broad and dorsomedially oriented, forming an angle of approximately 30° with the horizontal. The postzygapophyses are long and extend beyond the posterior margin of the centrum. The postzygapophyseal articular facets are ventrolaterally directed, forming an angle of approximately 20° with the horizontal. These articular facets are hidden below the prezygapophyses of the following vertebra. Epipophyses are absent from this vertebra. The neural spine is anteroposteriorly long and dorsoventrally short, being more than two times

longer than high (Table 1). This ratio is very unusual within Archosauria, except for the anterior-to-middle cervical vertebrae of *Qianosuchus mixtus* where the proportion ranges approximately from 2.0 to 2.5 (Li et al. 2006). Similar ratios, but less than two times longer than high, are observed for the aphanosaurians *Teleocrater rhadinus* (1.07–1.58; Nesbitt et al. 2017, 2018), *Yarasuchus deccanensis* (1.40–1.50; Sen 2005; Nesbitt et al. 2017) and *Spondylosoma absconditum* (1.34; Galton 2000; Nesbitt et al. 2017); and for the loricatans *Mandasuchus tanyauchen* (1.37–1.81; Butler et al. 2018) and *Trialetes romeri* (1.20; Lecuona et al. 2016). The anterior margin of the neural spine slants anterodorsally from its base forming an anterior overhang, giving the neural spine a trapezoidal outline in lateral view (Fig. 3A₂). This morphology is also present in the aphanosaurians *Teleocrater rhadinus* (Nesbitt et al. 2018), *Yarasuchus deccanensis* (Sen 2005), and *Spondylosoma absconditum* (Galton 2000); but also in the poposauroids *Qianosuchus mixtus* (Li et al. 2006) and *Xilousuchus sapingensis* (Nesbitt et al. 2010a), and the early diverging loricatan *Mandasuchus tanyauchen* (Butler et al. 2018). The distal end of the neural spine has a slight lateromedially rounded expansion with a rugose texture that ends on an almost flat dorsal margin (Fig. 3A₂). This condition is not interpreted as a true “spine table” in which the distal lateral expansion of the neural spine has an oval or a triangular shape in dorsal view (Nesbitt 2011). Typical spine tables are present in *Mandasuchus tanyauchen* (Butler et al. 2018), *Saurosuchus galilei* (Trotteyn et al. 2011), and *Batrachotomus kupferzellensis* (Gower and Schoch 2009). Nevertheless, the distal lateromedial expansion and rugose texture in the neural spine of *I. longicollum* gen. et sp. nov. resembles the condition of *Teleocrater rhadinus* (Nesbitt et al. 2018), *Yarasuchus deccanensis* (Sen 2005), *Spondylosoma absconditum* (Galton 2000) and *Xilousuchus sapingensis* (Nesbitt et al. 2010a).

The remaining cervical vertebrae include a set of two partially articulated and partially complete vertebrae (Fig. 4). These vertebrae are poorly preserved, because parts of the neural arches are broken and displaced, and the centra are mediolaterally compressed. As in the isolated cervical vertebra, the right lateral view is the most informative because the left side is hidden by several rib fragments. The anterior vertebra of this set has preserved the posterior half of the centrum, both postzygapophyses and an almost complete neural spine. The ventral surface of the centrum bears a well-defined midline ridge and its lateral surface has a shallow fossa, similar to those of the previously described vertebrae (Fig. 4A₂). The posterior articular surface anterodorsally slanted and has an elliptical outline in posterior view. The preserved postzygapophyses are notably long as in the other cervical vertebrae (Table 1). Epipophyses are absent from this vertebra. The neural spine lacks its anteriormost portion, but is dorsoventrally complete. As in the previously described isolated cervical vertebra, the neural spine is anteroposteriorly long, dorsoventrally short, and has a slight lateromedially rounded expansion with a rugose texture that ends on

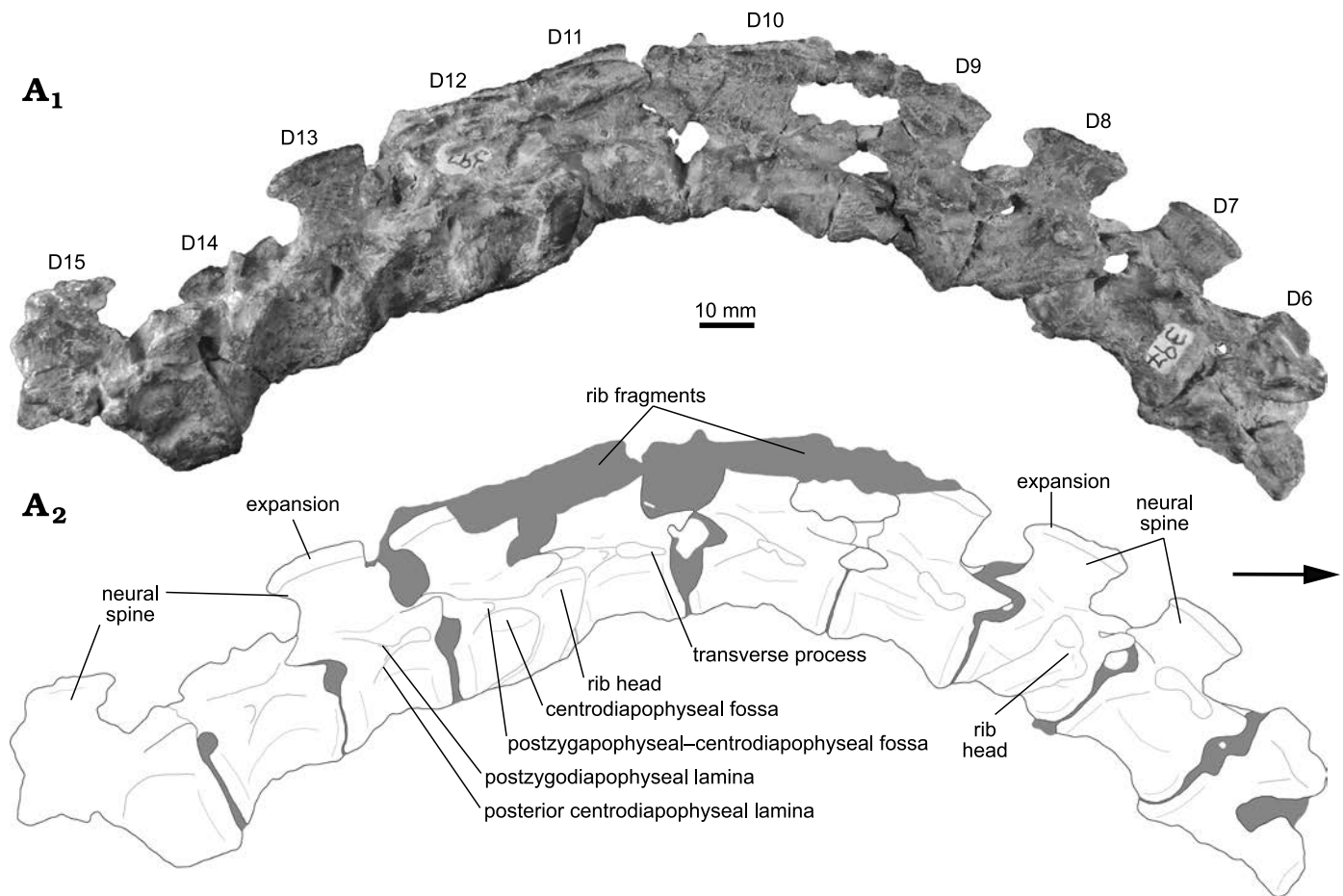


Fig. 5. Photograph (A₁) and interpretative drawing (A₂) of the articulated series of dorsal vertebrae (D6–D10) of the archosauriform *Incertovenator longicollum* gen. et sp. nov. (PVSJ 397) from Ischigualasto Formation (Carnian–Norian), Hoyada de Ischigualasto, Argentina; in right lateral view. Gray coloring represents broken bones and sediment. Arrow indicates anterior direction.

an almost flat dorsal margin (Fig. 4A₂). The posterior-most vertebra of the set preserves the anterior half of the centrum, the right prezygapophysis and a complete neural spine. The centrum has a midline ridge on its ventral surface similar to the ones present in the more anterior cervical vertebrae (Fig. 4A₂). The right diapophysis and parapophysis are placed on the anteroventral part of the neural arch and on the anterior portion of the centrum, respectively. These structures are separated from each other by approximately four millimeters. Their anterior and ventral location on the neural arch and centrum suggest these two vertebrae most likely correspond to the anterior-to-middle portion of the cervical series. As in the previous vertebrae, the horizontally oriented posterior centrodiapophyseal and posterior centroparapophyseal laminae delimit a fossa, which is deeper than in the preceding vertebrae (Fig. 4A₂). The lateral fossa becomes deeper beneath the posterior centrodiapophyseal ridge, forming a pit-like space. The right prezygapophysis is detached from the centrum and nearly touching the preceding right postzygapophysis. The neural spine is isolated from the rest of the vertebra. The neural spine is anteroposteriorly shorter than in the previously described cervical vertebrae (length/height ratio of approximately 1.8, Table 1). It has a lateromedially

rounded expansion with a rugose texture at its distal tip that ends on an almost flat dorsal margin. Contrasting with the other cervicals, the lateromedial expansion is slightly more developed, especially at the anteriormost and posteriormost ends of the neural spine. The dorsal margin of the neural spine projects anteriorly forming an anterior overhang giving it a trapezoidal outline in lateral view (Fig. 4).

Cervical rib: A single left cervical rib (Fig. 2) is preserved in articulation with the third cervical vertebrae. This rib is relatively anteroposteriorly short, only slightly longer than the vertebral centrum, and is oriented parallel to the longitudinal axis of the centrum. This general morphology is similar to those of most pseudosuchians (e.g., *Gracilisuchus stipanicorum*, Lecuona et al. 2017; *Ticinosuchus ferox*, Krebs 1965; *Mandasuchus tanyauchen*, Butler et al. 2018; *Postosuchus alisonae*, Peyer et al. 2008; *Sphenosuchus acutus*, Walker 1990; *Dibothrosuchus elaphros*, Wu and Chatterjee 1993; *Trialestes romeri*, Lecuona et al. 2016) but contrasts with the long and slender morphology of poposauroids (e.g., *Qianosuchus mixtus*, Li et al. 2006; *Xilousuchus sapingensis*, Nesbitt et al. 2010a) and most ornithomirans (e.g., *Lewisuchus admixtus*, Romer 1972; *Silesaurus opolensis*, Dzik 2003; *Eoraptor lunensis*, Sereno et al. 2012; *Coelo-*

Table 2. Selected measurements (in mm) of the dorsal vertebrae (D6–D15) of *Incertovenator longicollum* (PVSJ 397). All measurements are the maximum measurable. [] estimated measurement; * incomplete element; || an element (e.g., a vertebral centrum) that is not completely preserved (e.g., in anteroposterior length) but was measured nonetheless.

| | | D6 | D7 | D8 | D9 | D10 | D11 | D12 | D13 | D14 | D15 |
|-----------------------------|-------------------------------------|-----------------|------|----------------|------|------|--------|--------|-------|--------|--------|
| Centrum length | | 22.6 | 22.9 | 21.2 | 24.8 | 27.4 | 22.1 | 18.1 | 21.0 | 20.4 | 12.4* |
| Centrum length/height ratio | | – | 1.94 | 1.59 | 1.94 | 2.38 | 1.44 | 1.55 | 1.71 | 1.49 | – |
| Maximum height | | 30.3* | 34.5 | 35.1 | 35.1 | 33.7 | 35.2 | 32.7 | 34.8 | 28.3* | 35.5 |
| Anterior articular facet | height | 11.8 | 11.3 | 12.3 | 15.0 | 13.7 | 15.4 | [10.5] | 12.3 | 11.7 | 15.7 |
| | width | 9.3 | 11.2 | 11.4 | 10.9 | 9.4 | 6.9* | [8.8] | [8.5] | 11.3 | 14.2 |
| Posterior articular facet | height | 12.4 | 11.8 | 13.3 | 12.8 | 11.5 | [10.2] | 11.7 | 12.3 | 13.7 | – |
| | width | [9.3] | 11.5 | 8.8* [10.1] | 10.5 | 11.1 | 8.8 | [8.5] | 11.1 | 12.0 | – |
| Neural arch length | | 10.2* [20.2] | 22.0 | 22.3 | 22.9 | 23.7 | 23.1 | [17.6] | 20.1 | 18.8 | – |
| Neural spine | length | 14.3* | 17.4 | 19.9 | 17.2 | 13.5 | 19.3 | [20.7] | 18.2 | – | 14.6* |
| | height | – | 11.8 | 12.1 | 12.1 | 13.0 | 14.0 | 13.8 | 15.0 | 9.0* | 15.0 |
| | length/height ratio | – | 1.47 | 1.64 | 1.42 | 1.04 | 1.38 | [1.50] | 1.21 | – | – |
| | blade width | – | 1.96 | 2.08 | – | – | – | – | 2.47 | – | – |
| | distal lateromedial expansion width | – | 3.16 | 3.03 | – | – | – | – | 3.21 | – | – |
| Prezygapophyses length | | – | 11.2 | 11.2 | 10.4 | 11.6 | 9.7 | 10.4 | 10.3 | 8.7 | 9.6 |
| Postzygapophyses length | | – | 9.6 | 9.4 | 9.3 | 8.1 | 10.5 | 10.3 | 10.6 | [10.8] | – |
| Anterior neural canal | height | – | – | – | – | – | – | – | – | – | [4.81] |
| | width | – | – | – | – | – | – | – | – | – | [3.7] |
| Posterior neural canal | height | – | – | – | – | – | – | – | – | – | – |
| | width | – | – | – | – | – | – | – | – | – | – |

physis bauri, Colbert 1989). The tuberculum is slightly longer than the capitulum, and the two processes merge ventrolaterally with the rib shaft delimiting a vertebrocostal canal. The proximalmost part of both the tuberculum and capitulum is anteroposteriorly expanded with respect to the rest of the process. The rib bears a relatively long anterior process, representing approximately 20% of the total rib length, that projects anteriorly reaching the level of the posterior margin of the axis (Fig. 2A₃). Similar processes are found in suchians such as *Gracilisuchus stipanicorum* (Lecuona et al. 2017), *Ticinosuchus ferox* (Krebs 1965), *Xilousuchus sapingensis* (Nesbitt et al. 2011), *Mandasuchus tanyauchen* (Butler et al. 2018), *Hesperosuchus agilis* (Colbert 1952) and *Trialestes romeri* (Lecuona et al. 2016), among others; whereas in avemetarsalians are present in *Teleocrater rhadinus* (Nesbitt et al. 2018), *Eoraptor lunensis* (Serenó et al. 2012) and *Coelophysus bauri* (Colbert 1989). The posterior process of the rib is thin and its medial surface is dorsoventrally concave, giving it a C-shaped cross-section. This process extends posteriorly exceeding the posterior margin of the vertebral centrum.

Dorsal vertebrae: The preserved dorsal vertebrae (D) consist of an articulated series of ten vertebrae, interpreted ranging from D5/D6 to D14/D15 (see below; Fig. 5). The first and last vertebrae of this series are poorly preserved. D5/D6 lacks the anterior portion of the neural arch and its neural spine; whereas D14/D15 lacks the posterior half. The other vertebrae are complete and relatively well preserved, although some of them have considerable superficial weathering. Additionally, some articulated dorsal ribs are fragmentarily preserved. To simplify anatomical description of the series, the anteriormost vertebra will be considered as D6

and, therefore, the posteriormost vertebra as D15. The relative placement of the dorsal series within the axial skeleton was primarily determined based on the position of the parapophyses with respect to the inferred position of the neurocentral suture and diapophyses. The preserved dorsal vertebrae do not exhibit a migration of the parapophyses from the vertebral centrum to the neural arch, a feature only observed between the posterior cervicals and the anterior dorsal vertebrae in extant crocodylians and many crocodyliforms (Hoffstetter and Gasc 1968; Pol et al. 2012; Leardi et al. 2015), as well as in other archosaurs (*Teleocrater rhadinus*, *Marasuchus lilloensis*, *Lewisuchus admixtus*, *Gracilisuchus stipanicorum*, *Mandasuchus tanyauchen*, *Batrachotomus kupferzellensis*, *Dibothrosuchus elaphros*). Furthermore, D7 possesses its parapophyses well on the neural arch, nearly contacting the diapophyses, whereas already in D11 the apophyses are fused forming a single articular surface. Therefore, we interpreted the preserved series as ranging from the middle dorsal vertebrae to the posterior dorsal vertebrae.

Dorsal vertebral centra are anteroposteriorly shorter than cervical centra: the longest dorsal centrum of the series (D10) is approximately 25% shorter than the longest cervical centrum (C4; Tables 1, 2). The middle dorsal centra are anteroposteriorly longer than, or similar in length to, the anterior cervical centra in pseudosuchians such as *Riojasuchus tenuiceps* (Bonaparte 1971; Baczko and Ezcurra 2013), *Saurosuchus galilei* (Sill 1974; Trotteyn et al. 2011) and *Batrachotomus kupferzellensis* (Gower and Schoch 2009); whereas in others such as *Gracilisuchus stipanicorum* (Lecuona 2013; Lecuona et al. 2017), *Arizonasaurus babbitti* (Nesbitt 2005), *Effigia okeeffeae* (Nesbitt 2007), *Mandasuchus tanyauchen* (Butler et al. 2018) *Hesperosuchus agilis* (Colbert 1952) and

Trialestes romeri (Lecuona et al. 2016) the middle dorsal centra are anteroposteriorly shorter than the anterior cervical centra, similar to the condition observed in *I. longicollum* gen. et sp. nov. In *I. longicollum* gen. et sp. nov., all dorsal centra are anteroposteriorly longer than dorsoventrally high, with length/height ratios ranging from 1.44 to 2.38 along the entire series (Fig. 5; Table 2), similar to *Mandasuchus tanyauchen* and *Ticinosuchus ferox*. All dorsal centra are dorsoventrally higher than mediolaterally wide. This condition is similar to the one observed in *Riojasuchus tenuiceps* (Bonaparte 1971), *Saurosuchus galilei* (Trotteyn et al. 2011), *Dibothrosuchus elaphros* (Wu and Chatterjee 1993) and *Alligator mississippiensis* (Mook 1921), but contrasts with the condition in the poposauroids *Sillosuchus longicervix* (Alcober and Parrish 1997) and *Effigia okeeffeae* (Nesbitt 2007), in which the dorsal centra are mediolaterally wider than dorsoventrally high. Dorsal centra of *I. longicollum* gen. et sp. nov. are amphicoelous, with dorsoventrally higher than wide articular facets. In lateral view, the anterior and posterior articular facets are vertical, and the ventral surfaces of the centra are concave (Fig. 5). Contrasting with the condition described for the cervical centra, there are no depressions or fossae on the lateral surfaces of the dorsal centra. In ventral view, dorsal centra are strongly compressed so that they are very narrow at their midpoints (ranging approximately 3–5 mm). Ventral ridges or keels are absent from the ventral surfaces of the centra. Along the dorsal series there is a progressive increase in the anteroposterior length of the vertebral centra, starting from the anteriormost vertebra and reaching a maximum in the D10, followed by a progressive decrease in anteroposterior length towards the posterior end of the series (Fig. 5; Table 2). There are no remains of isolated parapophyses in the preserved dorsal centra, indicating that the fusion with the diapophyses took place in the preceding dorsal vertebrae.

The neural canal morphology can only be determined in D15, where it is elliptical in shape, with the dorsoventral axis being longer than the mediolateral one. In lateral view, the prezygapophyses are anteriorly or slightly anterodorsally projected, forming an angle of approximately 30° with the horizontal (Figs. 5, 6). In D7, the prezygapophyses lie in the same horizontal plane as the transverse process (Fig. 6), whereas in D13 they extend further dorsally than the diapophyses. In all dorsal vertebrae, the prezygapophyses project a short distance beyond the anterior margin of the centrum (Fig. 6) and have a subtriangular cross-section. The articular surfaces of the prezygapophyses have an ovate outline in dorsal view. These surfaces are flat and are inclined only slightly medially. There are no distinct prezygodiapophyseal or anterior centrodiapophyseal laminae on the preserved vertebrae.

In all dorsal vertebrae, the transverse processes project laterally in dorsal view and almost horizontally in anterior view. They have a subrectangular cross-section that is dorsally convex in lateral view. The posteroventral margin of the transverse processes supports a posterior centrodia-

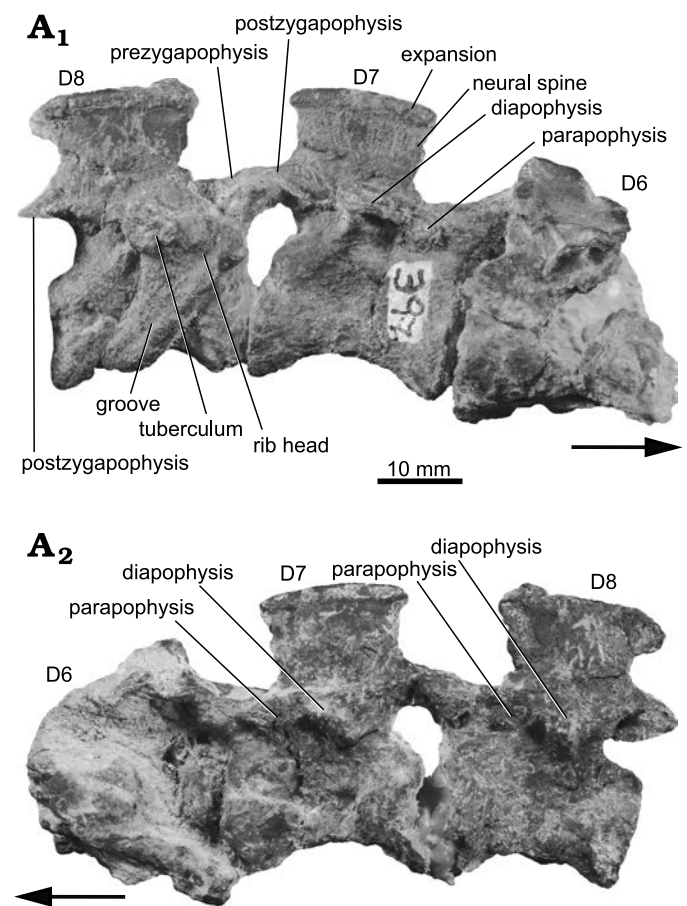


Fig. 6. Photographs of selected dorsal vertebrae (D6–D8) of the archosauriform *Incertovenator longicollum* gen. et sp. nov. (PVSJ 397) from Ischigualasto Formation (Carnian–Norian), Hoyada de Ischigualasto, Argentina; in right (A₁) and left (A₂) lateral views. Arrows indicate anterior direction.

pophyseal lamina, which forms the posterodorsal margin of a subtriangular, ventrally open centrodiapophyseal fossa, and the anteroventral margin of a small, shallow, posteriorly open postzygapophyseal–centrodiapophyseal fossa. These structures can be better appreciated in D11–D13 vertebrae, where there is less superficial weathering of the bone (Fig. 5A₂). The posterior margins of the diapophyses are linked to the ventral margins of the postzygapophyses by a well-developed postzygodiapophyseal lamina, which forms the dorsal border of the postzygapophyseal–centrodiapophyseal fossa. The postzygapophyses project shortly beyond the posterior margin of the centra. The articular surfaces of the postzygapophyses face ventrally, or slightly ventrolaterally, they are ovate in outline in ventral view and slightly concave. There are no hyosphene–hypantrum accessory articulations present in these vertebrae.

The neural spines are anteroposteriorly long, but relatively dorsoventrally low, approximately as high as the dorsal centra (Figs. 5, 6; Table 2), similar to the morphology of the cervical neural spines. The presence of dorsoventrally low neural spines in *I. longicollum* gen. et sp. nov. contrasts with the condition observed in some aphanosaurians (e.g., *Teleocrater*

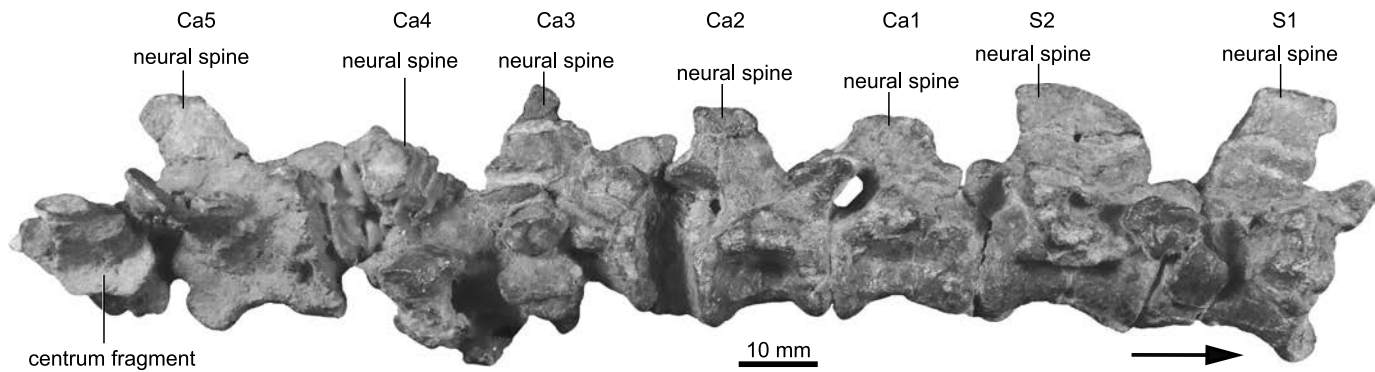


Fig. 7. Photograph of articulated series of sacral vertebrae (S1, S2) and anterior caudal vertebrae (Ca1–Ca5) of the archosauriform *Incertovenator longicollum* gen. et sp. nov. (PVSJ 397) from Ischigualasto Formation (Carnian–Norian), Hoyada de Ischigualasto, Argentina; in right lateral view. Arrow indicates anterior direction.

rhadinus, Nesbitt et al. 2018; *Yarasuchus deccanensis*, Sen 2005), gracilisuchids (e.g., *Gracilisuchus stipanicicorum*, Lecuona et al. 2017), poposauroids (e.g., *Qianosuchus mixtus*, Li et al. 2006; *Arizonasaurus babbitti*, Nesbitt 2005; *Xilousuchus sapingensis*, Nesbitt et al. 2010a), and loricatans (e.g., *Batrachotomus kupferzellensis*, Gower and Schoch 2009; *Postosuchus kirkpatricki*, Weinbaum 2013; *Dromicosuchus grillator*, Sues et al. 2003), in which the dorsal neural spines are dorsoventrally taller than anteroposteriorly long; but is similar to some dinosauiromorphs (e.g., *Marasuchus lilloensis*, Sereno and Arcucci 1994b; *Lewisuchus admixtus*, Bittencourt et al. 2015), crocodylomorphs (e.g., *Trialestes romeri*, Lecuona et al. 2016; *Terrestrisuchus gracilis*, Crush 1984) and the loricatan *Mandasuchus tanyauchen* (Butler et al. 2018). In lateral view, the neural spines form a trapezoidal plate that extends dorsally without any anterior or posterior inclination of its dorsoventral axis (Fig. 6). In lateral view, the anterior margins of the neural spines are straight, whereas the posterior and dorsal margins are gently curved. The anterior and posterior margins diverge as they extend dorsally. Along the dorsal series, the posterior margin of the neural spines becomes progressively more excavated towards the posteriormost vertebrae (Fig. 5). The curvature of the posterior margin produces an overhang of the posterodorsal tip of the neural spine that does not extend beyond the posterior margin of the vertebra (Figs. 5, 6). In anterior view, the neural spine is mediolaterally thin (less than 2 mm wide), but at its distal end it forms a rounded lateromedial expansion (Fig. 6). This lateromedial expansion is not, however, as prominent as those of *Parringtonia gracilis* (Nesbitt and Butler 2013), *Nundasuchus songeaensis* (Nesbitt et al. 2014), *Mandasuchus tanyauchen* (Butler et al. 2018), or *Batrachotomus kupferzellensis* (Gower and Schoch 2009). In dorsal view, the lateromedial expansion of the neural spines possesses a subrectangular outline, contrasting with the oval or subtriangular outline of the previously mentioned taxa.

Dorsal rib: The only remains of preserved dorsal ribs are proximal portions articulated with vertebrae D8 and D12 (Figs. 5A₂, 6A₁). The articular head of the rib is anteroposteriorly long, approximately half the length of the vertebral centrum, and its posterodorsal end is relatively expanded,

coinciding with the location of the tuberculum. The proximal portion of the rib shaft is mediolaterally flattened and subrectangular in cross-section, and it bears a very shallow dorsoventral groove on its posterior surface that extends along its entire length. Additionally, there are several middle-to-distal rib shaft fragments arranged in a parallel fashion that cover the left side of D9 to D13 (Fig. 5). We interpret these elements as vertebrocostal rib segments of the right side taphonomically displaced to the left side of the series.

Sacral vertebrae: Two articulated sacral vertebrae (S) are preserved in *Incertovenator longicollum* gen. et sp. nov., articulated with the caudal series (Figs. 7, 8). Both sacral vertebrae are mostly complete, lacking the distal portions of the neural spines and the sacral ribs. Only the proximalmost

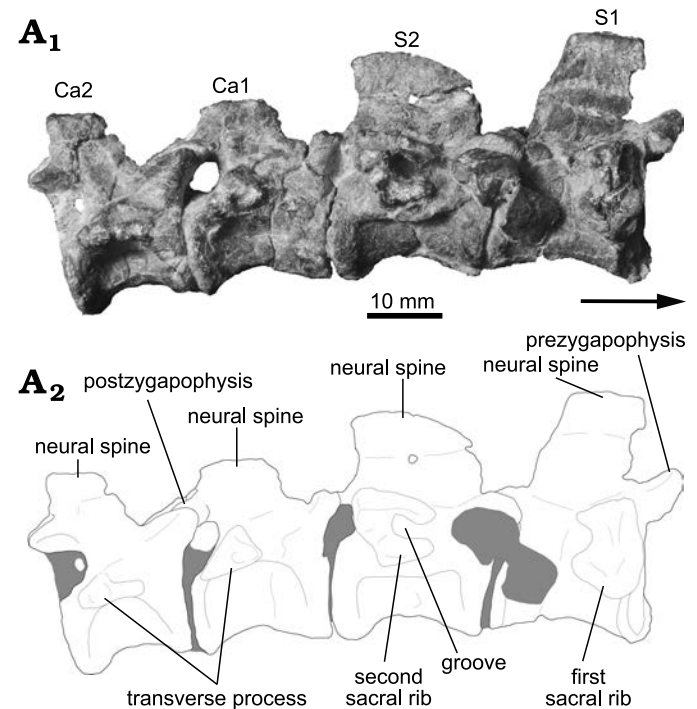


Fig. 8. Photograph (A₁) and interpretative drawing (A₂) of selected sacral (S1, S2) and caudal vertebrae (Ca1, Ca2) of the archosauriform *Incertovenator longicollum* gen. et sp. nov. (PVSJ 397) from Ischigualasto Formation (Carnian–Norian), Hoyada de Ischigualasto, Argentina; in right lateral view. Gray coloring represents bone fragments and sediment.

Table 3. Selected measurements (in mm) of the sacral (S1, S2) and caudal (Ca1–Ca5) vertebrae of *Incertovenator longicollum* (PVSJ 397). [] estimated measurement; * incomplete element.

| | S1 | S2 | Ca1 | Ca2 | Ca3 | Ca4 | Ca5 | |
|-----------------------------|--------|--------|---------|--------|---------|---------|---------|---------|
| Centrum length | 19.3 | 21.24 | 18.42 | 16.30 | 15.45 | 17.49 | 17.26 | |
| Centrum length/height ratio | 1.57 | 1.58 | 1.32 | 1.42 | 1.22 | 1.19 | [1.18] | |
| Maximum height | 33.84 | 31.44 | 26.02* | 27.78* | 30.27* | 28.98* | 29.36 | |
| Anterior articular facet | height | 14.24 | [13.93] | 12.16 | 13.02 | 12.69 | [14.27] | [14.60] |
| | width | 10.27 | 10.80 | 9.32 | 10.44 | 13.70 | 12.98 | 9.73 |
| Posterior articular facet | height | 12.29 | 13.46 | 13.93 | 11.48 | [14.60] | 14.67 | – |
| | width | 11.09 | 11.44 | 11.28 | 10.27 | 14.72 | 12.74 | – |
| Neural arch length | 15.10 | 14.76 | 16.61 | 13.15 | [12.86] | 12.00 | – | |
| Neural spine | length | 15.19* | 18.07 | 11.09 | 9.86 | 11.22 | 7.99 | 10.73 |
| | height | 15.26* | 11.44 | 6.15* | 8.40* | 8.78* | 12.28* | 8.44 |
| Prezygapophyses length | 8.22 | 9.84 | 8.47 | 6.45 | 9.52 | 8.94 | 7.36 | |
| Postzygapophyses length | 6.52 | [7.01] | 6.18 | 6.14 | 3.95 | – | 7.18 | |

portions of the right sacral ribs were preserved (but see ilium description). We infer that *I. longicollum* gen. et sp. nov. possesses two sacral vertebrae given that, when articulating the left ilium with the sacral vertebrae, there is no room to accommodate an additional vertebra on the medial wall of the ilium. Additionally, the morphology of the lateral extensions of the sacral ribs and their articular surfaces on the medial wall of the ilium are in agreement with the method for identifying the primordial sacral vertebrae proposed by Nesbitt (2011) (see ilium description). The sacral centra are clearly not co-ossified (Fig. 8), contrasting with the condition observed in poposauroids (e.g., *Sillosuchus longicervix*, Alcober and Parrish 1993; *Effigia okeeffeae*, Nesbitt 2007) and theropods (e.g., *Coelophysis bauri*, Colbert 1989).

The first primordial sacral centrum is anteroposteriorly longer than dorsoventrally high, with a length/height ratio of approximately 1.8 (Fig. 8; Table 3). The centrum is spool-shaped, with longitudinally concave lateral surfaces. The lateral surfaces are dorsoventrally convex and merge ventrally to form an acute angled border. There are no ventral midline structures nor evidence of any accessory vertebral lamina or ridges on the lateral surfaces. The anterior articular facet of the S1 centrum is mostly flat, or very gently concave, and subcircular in outline, whereas the posterior articular facet is obscured by the articulation with the second primordial sacral vertebra. The base of the transverse process extends along much of the dorsoventral height of the centrum and neural arch pedicel, being restricted to the anterior half of the vertebra. This process has a subquadrate outline in lateral view, with the ventral surface slightly longer than the dorsal one, and possesses a posteriorly directed concave notch. On the right lateral side, the transverse process articulates with the proximal-most portion of the first sacral rib (Fig. 8A₂), but the preservation of this structure is poor and precludes further description. The prezygapophyses project anterodorsally, exceed the anterior vertebral margin, and their articular facets are medially oriented. The postzygapophyses project posteriorly exceeding the posterior vertebral margin and their articular facets are ventrolaterally oriented. The neural spine is relatively long

anteroposteriorly, covering much of the neural arch length, it is distally incomplete and the preserved portion is dorsoventrally as high as the centrum (Fig. 8). The posterior margin of the neural spine slants anteriorly, whereas the anterior margin is mostly broken. In posterior view, the neural spine is blade-like and does not expand towards its distal end.

The second primordial sacral vertebra is similar to S1, although some differences are noticed. The lateral surface of S2 centrum is more longitudinally concave than S1, the transverse processes are located on the neural, arch and occupy most of the posterior half of the vertebra (Fig. 8). On the right lateral side, the proximal-most portion of the second sacral rib is articulating with the transverse process. The sacral rib is poorly preserved, but its anteriormost portion is dorsoventrally divided by a deep groove, approximately 3 mm wide, conferring it a “C shaped” cross-section (Fig. 8A₂). The prezygapophyses are more separated from each other as they diverge anterolaterally, contrasting with the prezygapophyses of the S1 that are more anteriorly projected. Finally, the morphology of the neural spine resembles that of the axial neural spine, where the distal margin is markedly dorsally convex and projects anteroventrally forming an arch (Fig. 8), nevertheless, this shape could be a preservational artifact.

Caudal vertebrae: Five articulated caudal vertebrae (Ca) are preserved in *Incertovenator longicollum* gen. et sp. nov. (Fig. 7). An additional centrum fragment is preserved attached to the posterior end of the last preserved caudal but is anatomically uninformative. The first two caudal vertebrae (Ca1 and Ca2) are well preserved and complete, only lacking the distal tips of their neural spines and transverse processes (Fig. 8). Ca3 and Ca4 are not as well preserved and their right lateral sides are covered by several bone fragments that obscure the vertebral surfaces. Ca5 is markedly compressed lateromedially and superficially weathered, although it has a complete neural spine (Fig. 7).

All vertebral centra are anteroposteriorly longer than dorsoventrally high, and the length/height ratio ranges between 1.4 and 1.2 (Figs. 7, 8; Table 3). This proportion changes more markedly between the first two caudals (1.3 and 1.4,

respectively) and between the second and third (after which the ratio is 1.2 or less). All centra are amphicoelous. The anterior and posterior articular facets of each centrum are dorsoventrally higher than mediolaterally wide. Distinct anterior chevron facets are absent in all preserved caudal vertebrae. Posterior chevron facets are only present in Ca3 and Ca4. However, these facets are only exposed in Ca4 because in Ca3 they are covered by the proximal portions of the chevron. In ventral view, the posterior chevron facets of Ca4 are beveled anteriorly. Chevrons are not preserved in any of the caudal vertebrae, with the exception of the small uninformative fragment attached to the Ca3.

The centra of Ca1–Ca4 are spool-shaped with longitudinally concave and dorsoventrally convex lateral surfaces that merge ventrally forming a smooth curve. The lateral surfaces of Ca1 and Ca2 centra are deeply excavated beneath the neural arch (Fig. 8). The ventral midline in Ca1–Ca4 lacks keels or grooves.

The transverse process is only partially preserved in the right side of Ca4. This process is positioned on the posteroventral corner of the neural arch, is subtriangular in cross-section and projects posterolaterally. The rest of the caudal vertebrae only preserve the proximal portion of the transverse processes. In Ca1 and Ca2 the proximal portion of the transverse processes are more anteriorly placed on the neural arches with respect to the condition in Ca4. These processes project laterally and slightly posteriorly, and have a subtriangular cross-section (Fig. 8A₂). The prezygapophyses are well preserved in all caudal vertebrae, they are triangular in cross-section and project anterodorsally exceeding the anterior vertebral margins. The articular facets of the prezygapophyses are dorsomedially oriented, with flat surfaces and an oval shape in dorsal view. There are no accessory vertebral laminae or ridges preserved on the lateral surfaces of the caudal vertebrae. The postzygapophyses are well preserved in all caudal vertebrae, except for Ca4. The postzygapophyses are placed on the ventral portion of the neural spines and project ventrally, and slightly posteriorly, exceeding their respective posterior vertebral margins. The articular facets of the postzygapophyses are ventrolaterally oriented and subcircularly shaped in ventral view.

Caudal neural spines are only partially represented in this series and it is only completely preserved in Ca5 (Fig. 7). The rest of the neural spines are in varying degrees of preservation. Ca1, Ca2 and Ca3 only preserve the base of the neural spine; while Ca4 preserves most of it, only lacking the distal tip. The neural spine of Ca5 is blade-like, it is as dorsoventrally high as the centrum and its dorsoventral axis is posteriorly slanted. In lateral view, the neural spine of Ca5 has a subrectangular outline, but its distal tip is rounded (Fig. 7). The neural spine of Ca4 lacks its distal tip, but is similar in shape to the neural spine of Ca5, only slightly dorsoventrally taller. The preserved caudal neural spines lack an accessory laminar process on the anterior face of the neural spine observed in taxa like *Qianosuchus mixtus* (Li et al. 2006; Nesbitt 2011), *Polonosuchus silesiacus* (Sulej 2005),

Ticinosuchus ferox (Krebs 1965), and *Terrestrisuchus gracilis* (Crush 1984). The bases of the neural spines progressively shift their position from a more anterior placement on the neural arch towards a more posterior one along the caudal series (Fig. 7). Likewise, the anteroposterior length of the bases of the neural spines becomes progressively shorter from the first caudal towards the fifth.

Pelvic girdle: The pelvic girdle of *Incertovenator longicollum* gen. et sp. nov. is only represented by an almost complete left ilium (Fig. 9). The ilium was not found articulated with the sacral vertebrae but was associated with the rest of the specimen.

Ilium: The ilium is relatively well preserved and lacks the distal tip of the preacetabular process and a small fragment on the ventralmost portion of the sheet of bone that connects the ischiadic peduncle with the ventral margin of the ilium. The ilium is anteroposteriorly elongated due to the marked extension of the iliac blade.

The iliac blade is as dorsoventrally high as the acetabulum and possesses a slightly concave dorsal margin in lateral view. The dorsal margin of the iliac blade possesses a rounded edge. The lateral surface of the iliac blade is smooth and is gently dorsoventrally convex. The iliac blade is separated from the acetabulum by a well-developed supraacetabular crest that projects laterally, and slightly ventrally, forming a deep acetabular roof. In lateral view, the supraacetabular crest curves anteroventrally reaching the anteriormost portion of the pubic peduncle (Fig. 9A₁, A₃). This anteroventral development of the supraacetabular crest resembles the conditions observed in some early crocodylomorphs (e.g., *Dibothrosuchus elaphros* and *Trialestes romeri*), but contrasts with the conditions of other early crocodylomorphs (e.g., *Dromicosuchus grillator* and *Terrestrisuchus gracilis*) in which the supraacetabular crest is relatively less expanded than in *Incertovenator longicollum* gen. et sp. nov. Posteriorly, the supraacetabular crest fades out dorsal to the end of the ischiadic peduncle. Dorsal to the supraacetabular crest, there is no development of a distinct vertical crest as in *Teleocrater rhadinus* (Nesbitt et al. 2018), *Yarasuchus deccanensis* (Sen 2005), *Asilisaurus kongwe* (Nesbitt et al. 2010b), *Arizonasaurus babbitti* (Nesbitt 2005), *Batrachotomus kupferzellensis* (Gower and Schoch 2009), *Rauisuchus tiradentes* (Lautenschlager and Rauhut 2015), or *Dromicosuchus grillator* (Sues et al. 2003). This crest is absent in taxa such as *Gracilisuchus stipanicorum* (Lecuona and Desojo 2011), *Turfanosuchus dabanensis* (Wu and Russel 2001), *Prestosuchus chiniquensis* (UFRGS-PV-0629-T, Mastrantonio 2010; Liparini and Schultz 2013), *Trialestes romeri* (PVL 3889, Lecuona et al. 2016), and *Dibothrosuchus elaphros* (Wu and Chatterjee 1993).

The preacetabular process is relatively anteroposteriorly long, representing approximately 29% (Table 4) of the total iliac blade extension (however, this proportion would be larger, considering that the preacetabular process is incomplete). Despite lacking its anterior tip, the preacetabular process projects anteriorly exceeding the anterior acetabular margin.

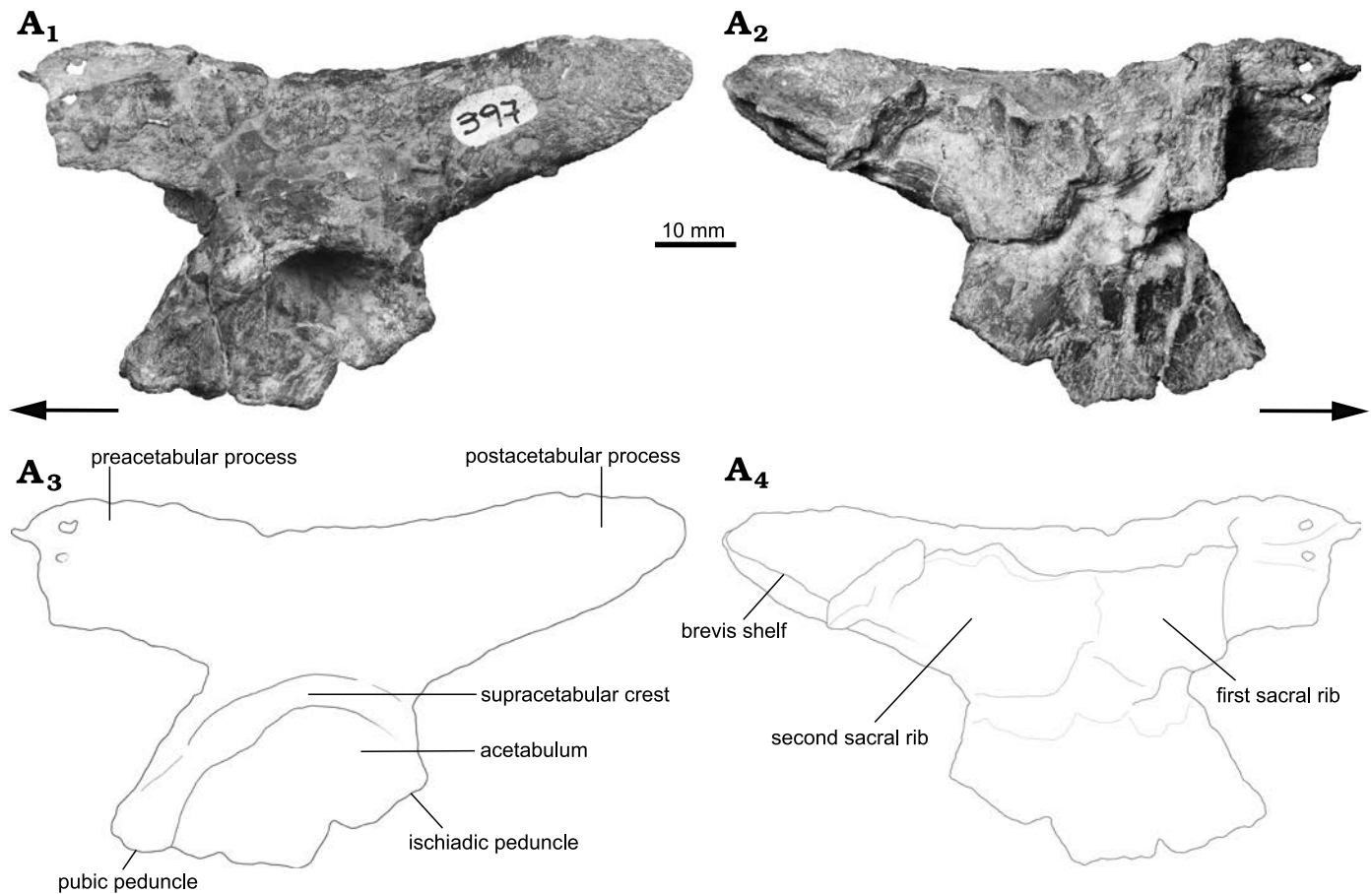


Fig. 9. Photographs (A₁, A₂) and interpretative drawings (A₃, A₄) of left ilium of the archosauriform *Incertovenator longicollum* gen. et sp. nov. (PVSJ 397) from Ischigualasto Formation (Carnian–Norian), Hoyada de Ischigualasto, Argentina; in lateral (A₁, A₃) and medial (A₂, A₄) views. Arrows indicate anterior direction.

Among pseudosuchians, the preacetabular also projects anteriorly exceeding the anterior acetabular margin in poposaurids (e.g., *Poposaurus gracilis*, Weinbaum and Hungerbühler 2007; *Effigia okeeffeae*, Nesbitt 2007; *Sillosuchus longicervix*, IY personal observation) and crocodylomorphs (e.g., CM 73372, JML personal observation; *Dromicosuchus grallator*, Sues et al. 2003; *Terrestrisuchus gracilis*, Crush 1984). Among avemetatarsalians, the preacetabular process projects anteriorly exceeding the anterior acetabular margin only in pterosaurs (e.g., *Dimorphodon macronyx*, Hyder et al. 2014; *Eudimorphodon ranzii*, Wellnhofer 2003) and dinosaurs (e.g., *Lesothosaurus diagnosticus*, Galton 1978; *Coelophysis bauri*, Colbert 1989). In dorsal view, the preacetabular process of *I. longicollum* gen. et sp. nov. is lateromedially narrow, approximately 3 mm wide. In lateral view, the proximal portion of the preacetabular process is relatively high, almost as high as the postacetabular process (Fig. 9A₁, A₃; Table 4), resembling the condition observed in *Poposaurus gracilis* (TTU-P 10419, Weinbaum and Hungerbühler 2007) and *Effigia okeeffeae* (Nesbitt 2007). In contrast, the proximal portion of the preacetabular process of the crocodylomorphs *Terrestrisuchus gracilis* (Crush 1984), *Trialestes romeri* (Lecuona et al. 2016), and *Dromicosuchus grallator* (Sues et al. 2003) is relatively short compared to the postacetabular process. Additionally,

in lateral view, the proximal portion of the preacetabular process is anterodorsally projected, resulting in a concave dorsal margin of the ilium that resembles the condition observed in taxa such as *Poposaurus gracilis* (“dorsal kink” sensu Parker and Nesbitt 2013; Weinbaum and Hungerbühler 2007),

Table 4. Selected measurements (in mm) of the left ilium of *Incertovenator longicollum* (PVSJ 397). * incomplete element.

| | |
|--|-------|
| Length | 86.5* |
| Maximum height | 44.6 |
| Iliac blade height (dorsal to acetabulum) | 15.7 |
| Length of the preacetabular process | 25.2* |
| Height of preacetabular process (proximal portion) | 19.2 |
| Length of the postacetabular process | 34.3 |
| Height of postacetabular process (proximal portion) | 21.4 |
| Width of the posterior end of the postacetabular process | 12.6 |
| Acetabular length | 33.1 |
| Acetabular height | 20.8 |
| Acetabular depth | 11.7 |
| Supraacetabular crest height | 6.9 |
| Length of the pubic peduncle | 8.2 |
| Depth of the pubic peduncle | 5.6 |
| Length of the ischiadic peduncle | 12.9 |
| Depth of the ischiadic peduncle | 5.9 |

Arizonasaurus babbitti (Nesbitt 2005), and *Protosuchus richardsoni* (Colbert and Mook 1951).

The postacetabular process is anteroposteriorly longer than the preacetabular process, comprising about 39% of the preserved length of the iliac blade, but considering that the preacetabular process is incomplete (Table 4). In lateral view, the postacetabular process projects posterodorsally and tapers at the posterior half, producing a long and rounded distal tip (Fig. 9A₁, A₃). In dorsal view, the dorsal margin of the postacetabular process is straight and mediolaterally narrow (approximately 2.6 mm). In ventral view, the ventral margin of the postacetabular process is also straight, but approximately two times wider than its dorsal margin. In lateral view, the ventral margin of the postacetabular process forms an obtuse angle with the posterior margin of the ischial peduncle (Fig. 9A₁, A₃). The lateral surface of this process is mostly smooth, however, towards the proximal portion of its dorsal margin, it has a striated area for the inferred origin site of the M. iliobtibialis (Schachner et al. 2011; Liparini and Schultz 2013). In medial view, the postacetabular process bears a ventromedially expanded shelf originated approximately at mid-dorsoventral height and runs parallel to the ventral margin of the postacetabular process (Fig. 9A₂, A₄). The shelf has a slightly concave ventral surface and an almost flat dorsal one.

The medial wall of the ilium bears a thin sheet of bone that runs from the junction of the preacetabular process and the pubic peduncle to the anterior half of the postacetabular process, dorsal to the ventromedially expanded shelf mentioned above (Fig. 9A₂). We interpret this sheet of bone as the fragmentary distal remains of the primordial sacral ribs articulated with the ilium (Fig. 9A₄), based on the method proposed by Nesbitt (2011) for identifying the primordial sacral vertebrae. A similar morphology of the primordial sacral ribs is present in taxa that retain the plesiomorphic condition for Archosauria (see Nesbitt 2011).

The pubic and ischiadic peduncles meet in the posterior half of the acetabulum at an angle of approximately 140° forming a triangular ventral margin. A triangular or convex ventral margin of the acetabulum is present in non-dinosaur avemetatarsalians (e.g., *Teleocrater rhadinus*, *Yarasuchus deccanensis*, *Asilisaurus kongwe*, *Silesaurus opolensis*, *Marasuchus lilloensis*) and in most pseudosuchians (e.g., *Turfanosuchus dabanensis*, *Arizonasaurus babbitti*, *Batrachotomus kupferzellensis*, *Postosuchus kirkpatricki*, *Dromicosuchus grillator*). On the contrary, the presence of a concave ventral acetabular margin is present in dinosaurs (e.g., *Lesothosaurus diagnosticus*, *Coelophysis bauri*), some poposauroids (e.g., *Poposaurus gracilis*, *Effigia okeeffeae*) and most early crocodylomorphs (e.g., *Trialestes romeri*, *Dibothrosuchus elaphros*, *Terrestriusuchus gracilis*, *Protosuchus richardsoni*). In lateral view, the anterior margin of the pubic peduncle is straight and dorsoventrally higher than the posterior margin of the ischial peduncle (Fig. 9). The pubic peduncle is anteroposteriorly longer than the ischiadic peduncle, covering more than half the length

of the ventral acetabular margin, as in *Silesaurus opolensis* and *Marasuchus lilloensis*. This contrasts with *Teleocrater rhadinus*, *Yarasuchus deccanensis*, *Asilisaurus kongwe*, and *Arizonasaurus babbitti* in which the ischiadic peduncle is anteroposteriorly longer than the pubic peduncle. In ventral view, the pubic peduncle broadens towards its anterior end forming a subquadrangular articular facet. The posterior margin of the ischiadic peduncle of *I. longicollum* gen. et sp. nov. is mainly vertical in lateral view and forms a gentle concavity where it meets the ventral margin of the postacetabular process (Fig. 9). This morphology contrasts with that of the pseudosuchians *Poposaurus gracilis*, *Prestosuchus chiniquensis*, *Saurosuchus galilei*, *Batrachotomus kupferzellensis*, *Postosuchus kirkpatricki*, CM 73372 (JML personal observation), and *Trialestes romeri* in which the concavity formed with the postacetabular process is deeper. In ventral view, the ischiadic peduncle broadens towards its posterior end forming an elliptical articular facet.

Remarks.—PVSJ 397 possesses the dark reddish-brown to greyish coloration typical of the Ischigualasto Formation attributed to extensive hematitic coatings and permineralizations (Colombi et al. 2012). General preservation is relatively poor because the specimen shows evidence of mediolateral compression and dorsoventral deformation by shear stress on some of its vertebral elements. Additionally, several elements display considerable cortical weathering and cracking.

All preserved centra are amphicoelous and there is no clear neurocentral suture observable in any vertebra. Despite this, it is noteworthy that in some vertebrae (especially in the isolated cervical vertebra) the neural arches are slightly detached from their respective centra at or near the neurocentral suture due to post-burial crushing. This separation gives the impression of an open neurocentral suture but contrasts with the posterior-most vertebrae that lack an open suture. Therefore, we consider that it is safe to assume closed neurocentral sutures along the preserved axial skeleton, thus suggesting a likely somatically mature specimen (Brochu 1996), although cautiously considering this criterion (Irmis 2007) because of the lack of a clear phylogenetic position. Comparisons of *Incertovenator longicollum* gen. et sp. nov. with other taxa known from the Ischigualasto Formation resulted in finding differences with all previously known species. For a comprehensive list of taxa used for comparison in this contribution see Appendix 1. Whereas the anatomical differences with most taxa are numerous and obvious, *I. longicollum* gen. et sp. nov. resembles in certain features the anatomy of *Trialestes romeri*. However, the preserved elements differ from those referred to *Trialestes romeri* in several respects, which are summarized at the end of the description.

Differences with *Trialestes romeri*: *Incertovenator longicollum* gen. et sp. nov. and *Trialestes romeri* (holotype PVL 2561 and referred specimen PVL 3889) are both from the Ischigualasto Formation and share a similar general size. *Incertovenator longicollum* gen. et sp. nov. and PVL 2561 come from the lower one-third of the Ischigualasto For-

mation at the Hoyada de Ischigualasto outcrops, whereas PVL 3889 comes from the outcrops immediately west of Cerro Las Lajas, approximately 260 m above the base of the Ischigualasto Formation (Desojo et al. 2020; Lecuona et al. 2016). Currently, *I. longicollum* gen. et sp. nov. is known from an incompletely preserved vertebral series and an ilium, with some of those bones having similar morphologies to those of the referred specimen of *Trialestes romeri* (PVL 3889; Lecuona et al. 2016). For a more thorough discussion about the referral of PVL 3889 to the hypodigm of *Trialestes romeri* see Lecuona et al. (2016) and Leardi et al. (2020). There are no overlapping elements between *I. longicollum* gen. et sp. nov. and the holotype specimen of *Trialestes romeri*. Therefore, in the following section we compare overlapping elements of *I. longicollum* gen. et sp. nov. and PVL 3889 (SOM: fig. 1, Supplementary Online Material available at http://app.pan.pl/SOM/app66-Yanez_etal_SOM.pdf).

Both specimens share anterior cervical vertebrae with greatly elongated centra and neural spines anteroposteriorly longer than high (centrum length/height ratios of the fourth cervical vertebrae for *I. longicollum* gen. et sp. nov. and PVL 3889 are approximately 2.98 and 2.43, respectively). However, the cervical vertebrae of PVL 3889 are almost 29% longer than those of *I. longicollum* gen. et sp. nov. (fourth cervical centrum length of 47.7 mm and 37.0 mm, respectively; SOM: fig. 1A₂, B₂). However, this size difference is not correlated with the pelvic girdle size, as the iliac length in PVL 3889 is virtually the same as in *I. longicollum* gen. et sp. nov. (87.4 mm and 86.5 mm, respectively; SOM: fig. 1A₄, B₄). This suggests that *I. longicollum* gen. et sp. nov. represents an individual with a body size similar to *Trialestes romeri* (PVL 3889), but with a shorter and lightly-built neck. Beyond the overall size difference, the cervical neural spines of *I. longicollum* gen. et sp. nov. are half the height when compared to those of PVL 3889 (neural spine length/height ratios of the fourth cervical vertebrae are approximately 2.41 and 1.20, respectively; SOM: fig. 1A₂, B₂). The cervical region of *I. longicollum* gen. et sp. nov. further differs from that of PVL 3889 in the presence of the following character states for the dataset used in the phylogenetic analysis (see below): anterior cervical neural spines with a rugose expansion at its distal end (char. 191: 3), anterior and middle post-axial cervical neural spines with an anterior overhang (char. 419: 1), cervical rib with posterior processes that exceeds the posterior articular facet of its corresponding vertebra. The dorsal vertebrae of *I. longicollum* gen. et sp. nov. also differ from those of PVL 3889 in several features, such as the presence of laterodistal expansions on the neural spines with a rounded dorsal margin (char. 197: 2), neural spines with a posterodorsal tip overhanging the neural arch, and absence of ventral paramedian ridges on the vertebral centra of the more posterior anterior-dorsals (SOM: fig. 1A₁, B₁). The sacral vertebral centra of *I. longicollum* gen. et sp. nov. differ from those of PVL 3889 in that they are not fused to each other, are taller than broad, and transversely constricted in ventral view (SOM: fig. 1A₃, B₃). Furthermore,

the sacral vertebral centra of *I. longicollum* gen. et sp. nov. are almost 85% longer than those of PVL 3889.

Regarding the ilium, *Incertovenator longicollum* gen. et sp. nov. differs from PVL 3889 in that it possesses a concave dorsal margin of the iliac blade in lateral view, the preacetabular process is dorsoventrally higher at mid length, and the dorsal margin of the preacetabular process is laterally arched in dorsal view (SOM: fig. 1A₄, B₄). The distal half of the postacetabular process in *I. longicollum* gen. et sp. nov. tapers distally to a rounded point, whereas in PVL 3889 the distal end of the postacetabular process is blunt. In *I. longicollum* gen. et sp. nov., the ventromedially expanded shelf of the postacetabular process originates approximately at mid-dorsoventral height, whereas in PVL 3889 this structure originates from the ventral margin. In this sense, the medial shelf in *I. longicollum* gen. et sp. nov. projects forming an almost horizontal platform, whereas in PVL 3889 the medial shelf projects mostly ventrally and only slightly medially. The anteroventral extension of the supraacetabular crest is more developed onto the lateral surface of the pubic peduncle in *I. longicollum* gen. et sp. nov. than in PVL 3889 (SOM: fig. 1A₄, B₄). On the other hand, the ischiadic peduncle of *I. longicollum* gen. et sp. nov. is oriented vertically in lateral view, whereas in PVL 3889 is posteroventrally directed (SOM: fig. 1A₄, B₄). Finally, the ilium of *I. longicollum* gen. et sp. nov. possesses a ventral margin with a convex (closed) acetabulum, whereas in PVL 3889 the ventral acetabular margin is partially concave (open), although we do not discard the possibility of a missing fragment of bone in PVL 3889 due to preservation or overpreparation (as similarly mentioned by Lecuona et al. 2016).

Stratigraphic and geographic range.—Type locality and horizon only.

Discussion

Phylogenetic relationships.—In order to assess the phylogenetic affinities of *Incertovenator longicollum* gen. et sp. nov. (PVSJ 397) we included it in a parsimony analysis using the data matrix of Nesbitt et al. (2017). We also incorporated *Trialestes romeri* (after Lecuona et al. 2016) and *Mandasuchus tanyauchen* (after Butler et al. 2018) to this data set (see SOM for further details). The final matrix consisted of 85 taxa and 419 characters. The fragmentary nature of *I. longicollum* gen. et sp. nov. allowed for only 8.6% of the entries to be scored.

We conducted an equally weighted parsimony analysis in TNT 1.5 (Goloboff et al. 2008; Goloboff and Catalano 2016) performing 1000 replicates of Wagner trees followed by TBR branch swapping. The best trees obtained from the replicates were subjected to a final round of TBR branch swapping. Decay indices (Bremer support values) were calculated using the script “bremsup.run” (see SOM) and a bootstrap resampling analysis, using 10 000 pseudorepli-

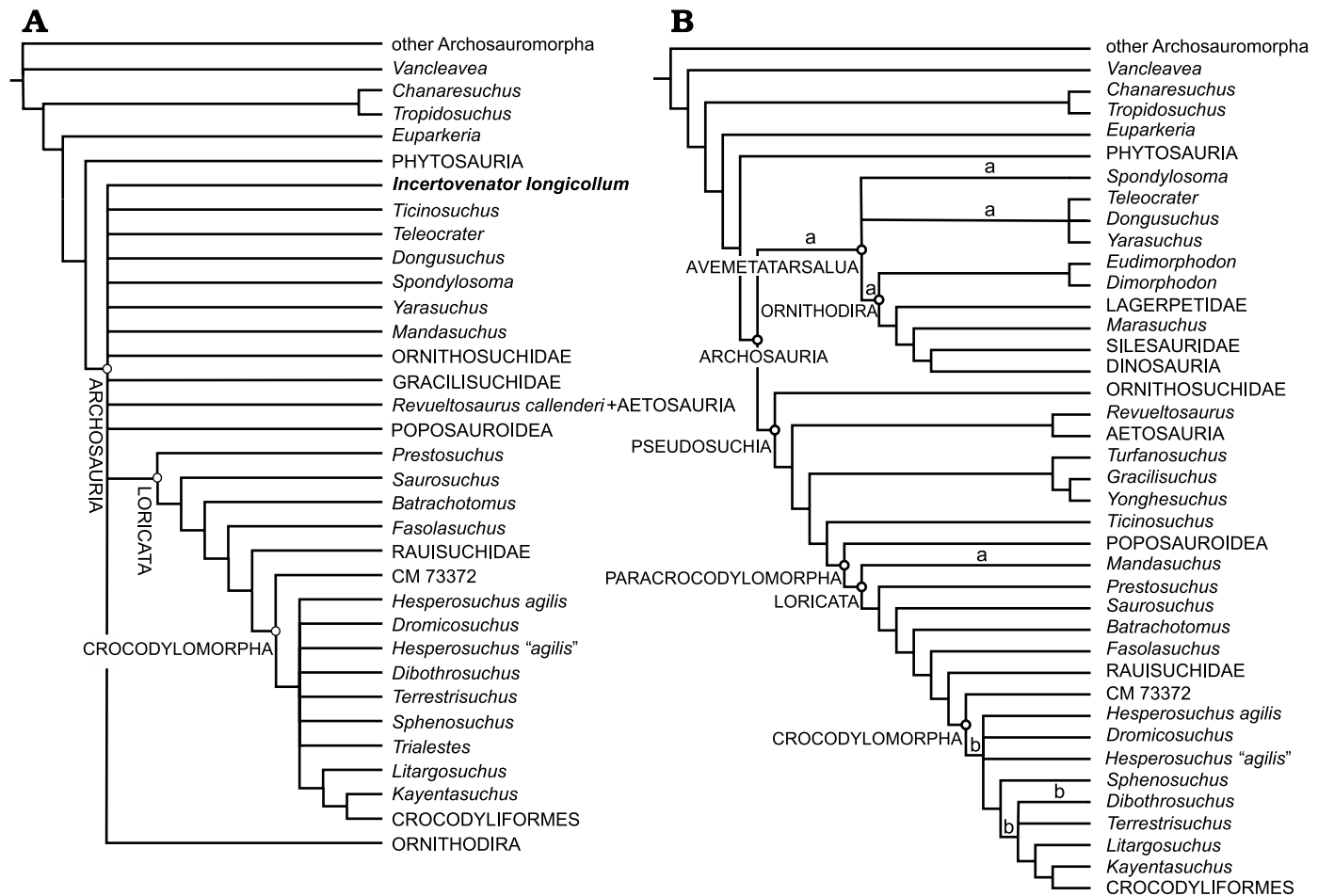


Fig. 10. Strict consensus tree of the 1188 MPTs (A), and reduced strict consensus tree of the 1188 MPTs (B) showing the alternative phylogenetic positions for *Incertovenator longicollum* gen. et sp. nov. ("a") and the combined OTU for *Trialestes romeri* ("b"). Note that in the strict consensus trees the clade Aphanosauria is not exactly recovered as defined by Nesbitt et al. (2017) (*Spondylosoma* + *Teleocrater* + *Dongusuchus* + *Yarasuchus*) due to the multiple alternative phylogenetic positions of *Incertovenator longicollum* gen. et sp. nov. and *Spondylosoma absconditum*.

cates, was performed calculating both absolute and GC frequencies (Goloboff et al. 2003).

The analysis recovered 1188 MPTs of 1401 steps (CI = 0.350, RI = 0.779) and the best score was found in 641 hits of the 1000 replicates. The strict consensus tree (Fig. 10A) depicts *I. longicollum* gen. et sp. nov. in a large polytomy together with *Mandasuchus lilloensis*, *Teleocrater rhadinus*, *Yarasuchus deccanensis*, *Spondylosoma absconditum*, *Dongusuchus efremovi*, *Ticinosuchus ferox*, Ornithodira, Ornithosuchidae, *Revueltosaurus callenderi* + Aetosauria, Gracilisuchidae, Popsauroidea, and the rest of Loricata (see SOM: fig. 2 for the strict consensus tree with supporting values). The polytomy is produced by the multiple alternative positions of *I. longicollum* gen. et sp. nov., thus ignoring these different positions in a reduced strict consensus, resolves the relationships among the early diverging nodes of Archosauria (Fig. 10B), in general agreement with the results of previous versions of this dataset (Nesbitt 2011; Butler et al. 2014, 2018; Lecuona et al. 2016; Nesbitt et al. 2017).

Incertovenator longicollum gen. et sp. nov. takes alternative most-parsimonious phylogenetic positions among the early diverging nodes of Archosauria (Fig. 10B). One of the

obtained positions places *I. longicollum* gen. et sp. nov. as the sister taxon of the loricatan *Mandasuchus tanyauchen*, whereas the other positions depict *I. longicollum* gen. et sp. nov. in different early diverging nodes of Avemetatarsalia. The latter set of positions depicts *I. longicollum* gen. et sp. nov. alternatively as sister taxon to Aphanosauria, Avemetatarsalia, and Ornithodira. A similar set of alternative positions is found for *Spondylosoma absconditum*, which is depicted closer to either of these three groups (Avemetatarsalia, Ornithodira, Aphanosauria) and/or as the sister taxon of *I. longicollum* gen. et sp. nov.

Incertovenator longicollum gen. et sp. nov. possesses a combination of vertebral character states that support its placement as an early diverging avemetatarsalian as they are also present in at least one aphanosaurian taxon: anterior to middle cervical vertebrae longer than the mid-dorsal vertebrae (char. 181: 1; present in *Yarasuchus deccanensis*, *Teleocrater rhadinus*, and *Spondylosoma absconditum*), cervical neural spines with a rugose expansion at their distal ends (char. 191: 3; present in *Teleocrater rhadinus* and *Yarasuchus deccanensis*), distal expansion on the dorsal vertebrae neural spines with a rounded dorsal margin (char. 197: 2; also

present in *Yarasuchus deccanensis*) and anterior to middle cervical neural spines with an anterodorsally inclined anterior margin (char. 419: 1; present in *Teleocrater rhadinus*, *Yarasuchus deccanensis*, and *Spondylosoma absconditum*). In fact, the latter character state was found as the only unambiguous synapomorphy of Aphanosauria by Nesbitt et al. (2017). Similarly, the position of *I. longicollum* gen. et sp. nov. as the sister taxon of the loricatan *Mandasuchus tanyauchen* is supported by derived features of the cervical region: the presence of a convex dorsal margin on the axial neural spine (char. 179: 1) and an anterodorsally inclined anterior margin of the cervical vertebrae (char. 419: 1).

Alternative phylogenetic positions of *Incertovenator longicollum* gen. et sp. nov.—The cervicodorsal vertebral features mentioned above, however, are not exclusive of aphanosaurians or *Mandasuchus tanyauchen*. Firstly, *I. longicollum* gen. et sp. nov. shares the presence of elongated cervical vertebrae (char. 181: 1) with more crown-ward members of Ornithodira (pterosaurs, silesaurids), with several suchians (*Gracilisuchus stipanicorum*, early poposauroids, the crocodylomorph *Trialestes romeri*), and with the non-archosaurian archosauriform *Tropidosuchus romeri*. Secondly, *I. longicollum* gen. et sp. nov. also shares the presence of an anterodorsally inclined anterior margin of the cervical vertebrae (char. 419: 1) mentioned above for *Tropidosuchus romeri*, gracilisuchids, *Qianosuchus mixtus*, and crocodylomorphs (e.g., *Terrestriusuchus gracilis* and *Dibothrosuchus elaphros*). Thirdly, *I. longicollum* gen. et sp. nov. shares with the ornithodirans *Marasuchus lilloensis*, *Lewisuchus admixtus*, and *Silesaurus opolensis*, and with the suchian *Ticinosuchus ferox* the presence of a convex dorsal margin on the axial neural spine (char. 179: 1); a character state that was reported as an ambiguous synapomorphy of Ornithodira by Nesbitt et al. (2017).

On the other hand, the iliac morphology of *I. longicollum* gen. et sp. nov. resembles the condition of early crocodylomorphs, late surviving poposauroids, pterosaurs and dinosaurs in having a long preacetabular process that extends anterior to the acetabulum (char. 269: 1). This condition differs from that of *Teleocrater rhadinus* and *Yarasuchus deccanensis*, as these taxa have a short preacetabular process that does not exceed the anterior acetabular margin. Unlike these early diverging avemetatarsalians, *I. longicollum* gen. et sp. nov. also lacks several features present in them: cervical epiphyses (char. 186: 1), a crest dorsal to the supraacetabular crest of the ilium (char. 265: 2), and a distinct notch on the ischial peduncle of the ilium (char. 414: 1).

The conflictive distribution of character states results not only in the uncertainty regarding the phylogenetic affinities of *I. longicollum* gen. et sp. nov., but also in the low support values for multiple nodes within Archosauria in our analysis (SOM: fig. 2). The similarities noted above for multiple character states (particularly those referring to the cervicodorsal region and iliac morphology) between *I. longicollum* gen. et sp. nov. and certain ornithodirans and

pseudosuchians, prompted us to further evaluate alternative phylogenetic positions that were marginally suboptimal (up to two steps). We implemented a script for TNT (see “swap-taxon.run” in SOM) to test the different positions that *I. longicollum* gen. et sp. nov. can take and that would imply one or two extra steps. For each of these positions we set up a monophyly constraint and ran a heuristic tree search to find the optimal topologies under such constraint (with identical tree search settings as the unconstrained analysis). Finally, we evaluated which characters supported the alternative positions of *I. longicollum* gen. et sp. nov. in comparison with that of the unconstrained MPTs (using the TNT script “compare.run”; see SOM).

The results of the exploration of suboptimal positions show *I. longicollum* gen. et sp. nov. in three main sets of phylogenetic placements within Archosauria, as well as one position outside this clade (Fig. 11). The first set of topologies places *I. longicollum* gen. et sp. nov. among early diverging nodes of Ornithodira, either as the sister taxon of Pterosauria (one extra step) or Dinosauromorpha (two extra steps), and several nodes within the latter clade (e.g., Lagerpetidae, *Dromomeron* spp., Dinosauriformes, dinosauriforms closer to Dinosauria than to *Marasuchus lilloensis*). The character states that favor these suboptimal positions are the presence of a long preacetabular process of the ilium (char. 269: 1; shared between *I. longicollum* gen. et sp. nov. and pterosaurs) and the presence of a convex dorsal margin of the axial neural spine (char. 179: 1; shared between *I. longicollum* gen. et sp. nov. and the mentioned dinosauriforms).

The second set of topologies corresponds to the alternative suboptimal positions that *I. longicollum* gen. et sp. nov. takes among successive nodes, from one node more derived than Suchia (two extra steps), as the sister taxon of Gracilisuchidae (one extra step), and up to the base of Loricata (two extra steps; Fig. 11). The character states that favor these resolutions are the presence of an anterodorsally inclined anterior margin of the cervical vertebrae (char. 419: 1; shared between *I. longicollum* gen. et sp. nov. and gracilisuchids) and the absence of a crest dorsal to the supraacetabular crest of the ilium (char. 265: 0; shared between *I. longicollum* gen. et sp. nov. and many of the taxa close to the above-mentioned nodes).

The third set of topologies corresponds to the alternative suboptimal positions that *I. longicollum* gen. et sp. nov. takes among early diverging Crocodylomorpha, in several nodes between one node closer to crocodyliforms than the base of Crocodylomorpha up to the base of the clade that comprises *Dibothrosuchus elaphros*, *Terrestriusuchus gracilis*, *Litargosuchus leptorhynchus* and taxa more closely related to crocodylomorphs (two extra steps; Fig. 11). It is noteworthy that several of these alternative positions are also taken by *Trialestes romeri* in some of the possible iterations. When this happens, *I. longicollum* gen. et sp. nov. and *Trialestes romeri* are recovered as sister taxa among those nodes in some resolutions (see in Fig. 11 where “b” coincides with the light gray circle). *Incertovenator longicollum*

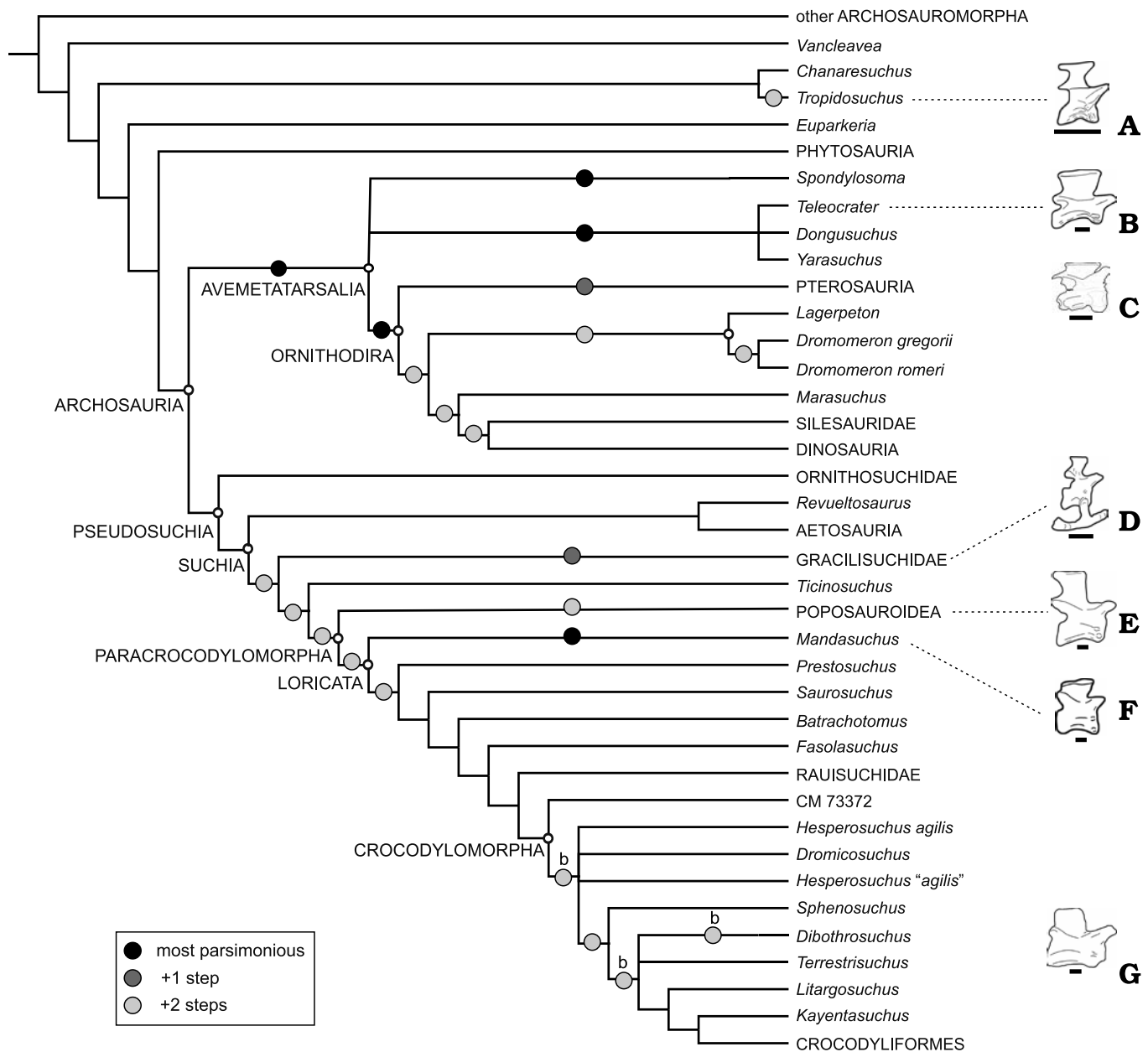


Fig. 11. Reduced strict consensus tree of the 1188 MPTs depicting alternative most-parsimonious phylogenetic positions (solid black circles) and suboptimal alternative positions of one extra step and two extra steps for *Incertovenator longicollum* gen. et sp. nov.; "b" represents the alternative most-parsimonious positions for *Trialestes romeri* (combined OTU). Schematic drawings of anterior cervical vertebrae in right lateral view of selected taxa with elongated necks: *Tropidosuchus romeri* (A; modified from Arcucci 1990), *Teleocrater rhadinus* NMT RB505 (B), *Incertovenator longicollum* gen. et sp. nov. PVSJ 397 (C), *Gracilisuchus stipanicorum* PVL 4597 (D; modified from Lecuona et al. 2017), *Xilousuchus sapingensis* IVPP V6026 (E), *Mandasuchus tanyauchen* NHMUK PV R6792 (F), *Trialestes romeri* PVL 3889 (G). E–G are mirrored for comparison. Scale bars 10 mm.

gen. et sp. nov. shares with crocodylomorphs the presence of a long preacetabular process of the ilium (char. 269: 1) and shares with *Trialestes romeri* the absence of a crest dorsal to the supraacetabular crest of the ilium (char. 265: 0).

Finally, *I. longicollum* gen. et sp. nov. is recovered in an additional alternative suboptimal position as the sister taxon of the non-archosaurian archosauriform *Tropidosuchus* (two extra steps; Fig. 11). This position is supported by the shared presence of an anterodorsally inclined anterior margin of the cervical vertebrae (char. 419: 1).

Convergences in archosaur cervical region.—These phylogenetic analyses based on the dataset of Nesbitt et al. (2017) reveal two major issues. First, there is uncertainty in the phylogenetic affinities of *Incertovenator longicollum* gen. et sp. nov. not only because of the fragmentary nature of the specimen and the lack of preservation of certain anatomical regions that would be key for defining its affinities, but also due to the mosaic combination of character states in the axial skeleton and ilium. At the moment, *I. longicollum* gen. et sp. nov. is most parsimoniously interpreted as either an early avemetatarsalian or as an early diverging loricatan from the

Ischigualasto Formation. However, it possesses clear derived similarities in the axial morphology that are shared with other groups of avemetatarsalians (e.g., dinosauromorphs, pterosaurs), pseudosuchians (e.g., Gracilisuchidae, *Trialestes romeri*), or the early archosauriform *Tropidosuchus romeri*. The iliac morphology of *I. longicollum* gen. et sp. nov. greatly diverges from that of the above-mentioned taxa and resembles that of most non-crocodyliform crocodylomorphs.

The second issue that the exploratory analyses reveal, is that the alternative phylogenetic affinities of *I. longicollum* gen. et sp. nov. among multiple and distantly related archosaur clades, are also caused because certain features of the axial skeleton (in particular cervical morphology) evolved multiple times independently in different clades of Avemetatarsalia and Pseudosuchia during the archosaur radiation. For instance, the clade Aphanosauria, Gracilisuchidae, and early poposauroids share the derived combination of some or all of the following character states: elongated cervical vertebrae, anteriorly slanted cervical neural spines, and incipiently developed spine tables in cervical neural spines. Interestingly, some or all of those character states are also present in the loricatans *Mandasuchus tanyauchen* and *Trialestes romeri*, and in the proterochampsian *Tropidosuchus romeri*. The functional implications of this peculiar pattern of elongated necks with modified neural spines (Fig. 11) have not been explored to date, but it seems that the elongation of the neck was repeatedly associated with modifications of the epaxial bony structures (and possibly the correlated muscles and/or ligaments; Tsuihiji 2005; Organ 2006). These epaxial changes may have been related to mobility or strengthening requirements of an elongated cervical region (Tsuihiji 2004; Molnar et al. 2014; Kambic et al. 2017). The repeated instances of convergences in this aspect of the body plan seem to be restricted to lineages of small-sized predators that appeared during the evolutionary radiation of Archosauromorpha between the late Middle to the early Late Triassic.

Conclusions

Incertovenator longicollum gen. et sp. nov. (PVSJ 397) represents a new taxon from the Ischigualasto Formation that increases the diversity of a key faunal assemblage for understanding archosaur radiation during the Late Triassic. The new taxon is characterized by a unique and conflictive combination of cervical and pelvic character states that are typically present in either early avemetatarsalians, early suchians and/or non-crocodyliform crocodylomorphs. *Incertovenator longicollum* gen. et sp. nov. possesses elongated cervical vertebrae (with centra more than two times longer than high), dorsoventrally short and anteroposteriorly long anterior cervical neural spines with a distal rugose expansion and an anteriorly slanted anterior margin. Additionally, *I. longicollum* gen. et sp. nov. has a long preacetabular process that extends beyond the anterior acetabular margin.

Our phylogenetic analysis recovers the new taxon in the most parsimonious trees as either an early avemetatarsalian or a pseudosuchian closely related to *Mandasuchus tanyauchen*. The exploration of alternative suboptimal topologies revealed possible affinities with different lineages of Ornithodira, but also with early suchians or crocodylomorphs. The reason underlying these disparate positions is that these phylogenetically distant lineages of archosauriforms convergently acquired a set of features in the cervical region that reflect elongated necks with possibly associated modifications of certain epaxial structure, related to either mobility or strengthening of this region. Regardless of the exact relationships of *I. longicollum* gen. et sp. nov., the current analysis agrees on the fundamental structure of the relationships of early archosaurs and their close relatives. Future work in the Ischigualasto Formation and new specimens of *I. longicollum* gen. et sp. nov. are needed to clarify its phylogenetic affinities and the palaeobiology of the taxon.

Acknowledgements

We thank Martín Ezcurra and Federico Agnolin (both Museo Argentino de Ciencias Naturales “Bernardino Rivadavia”, Ciudad Autónoma de Buenos Aires, Argentina) for valuable discussions and interpretations about the osteology of the specimen described in this contribution. We extend our sincere gratitude to Agustina Lecuona (Instituto de Investigación en Paleobiología y Geología, UNRN, Río Negro, Argentina) and Sterling Nesbitt (Virginia Tech, Blacksburg, USA) for kindly reviewing this work and whose comments and suggestions greatly improved the quality of this manuscript. We further thank Sterling Nesbitt for providing the data matrix with the character codings of *Mandasuchus tanyauchen* used for the phylogenetic analyses. We also thank Diego Abelín and Cecilia Apaldetti (both PVSJ) for mechanical preparation of the specimen and assistance in preparing some of the figures, respectively. We are grateful to the Instituto y Museo de Ciencias Naturales of the Universidad Nacional de San Juan for its continued support to our research. We also thank the Willi Hennig Society for making TNT 1.5 software freely available. This research was made possible by a Consejo Nacional de Investigaciones Científicas y Técnicas (CONICET) Doctoral Fellowship to IY. This is JML’s R-363 contribution to the Instituto de Estudios Andinos Don Pablo Groeber.

References

- Alcober, O. 2000. Redescription of the skull of *Saurosuchus galilei* (Archosauria: Rauisuchidae). *Journal of Vertebrate Paleontology* 20: 302–316.
- Alcober, O. and Parrish, J.M. 1997. A new poposaurid from the Upper Triassic of Argentina. *Journal of Vertebrate Paleontology* 17: 548–556.
- Arcucci, A.B., Marsicano, C.A., and Caselli, A.T. 2004. Tetrapod association and palaeoenvironment of the Los Colorados Formation (Argentina): a significant sample from Western Gondwana at the end of the Triassic. *Geobios* 37: 557–568.
- Baczko, M.B. von and Ezcurra, M.D. 2013. Ornithosuchidae: a group of Triassic archosaurs with a unique ankle joint. *Geological Society, London, Special Publications* 379: 187–202.
- Baczko, M.B. von, Desojo, J.B., and Pol, D. 2014. Anatomy and phylogenetic position of *Venaticosuchus rusconii* Bonaparte, 1970 (Archosaur-

- ria, Pseudosuchia), from the Ischigualasto Formation (Late Triassic), La Rioja, Argentina. *Journal of Vertebrate Paleontology* 34: 1342–1356.
- Benton, M.J. and Clark, J.M. 1988. Archosaur phylogeny and the relationships of the Crocodylia. In: M.J. Benton (ed.), *The Phylogeny and Classification of the Tetrapods*. Vol. 1. Amphibians, Reptiles, Birds. *Systematics Association Special Volume* 35A: 295–338.
- Benton, M.J. and Walker, A.D. 2002. *Erpetosuchus*, a crocodile-like basal archosaur from the Late Triassic of Elgin, Scotland. *Zoological Journal of the Linnean Society* 136: 25–47.
- Bittencourt, J.S., Arcucci, A.B., Marsicano, C.A., and Langer, M.C. 2015. Osteology of the Middle Triassic archosaur *Lewisuchus admixtus* Romer (Chañares Formation, Argentina), its inclusivity, and relationships amongst early dinosauroforms. *Journal of Systematic Palaeontology* 13: 189–219.
- Bonaparte, J.F. 1970. Annotated list of the South American Triassic tetrapods. In: S.H. Haughton (ed.), *Proceedings and Papers of the Second Gondwana Symposium*, 665–682. Council of Scientific and Industrial Research, Cape Town, Johannesburg.
- Bonaparte, J.F. 1971. Los tetrapodos del sector superior de la formación Los Colorados, La Rioja, Argentina (Triásico Superior) I parte. *Opera Lilloana* 22: 1–183.
- Bonaparte, J.F. 1978. Tecodontes: clasificación. In: J.F. Bonaparte (ed.), *El Mesozoico de América del Sur y sus tetrápodos. Capítulo XVIII*, 263–307. Opera Lilloana, Tucumán.
- Bonaparte, J.F. 1981. Descripción de *Fasolasuchus tenax* y su significado en la sistemática y evolución de los Thecodontia. *Revista del Museo Argentino de Ciencias Naturales "Bernardino Rivadavia"* 3: 55–101.
- Bonaparte, J.F. 1982. Faunal replacement in the Triassic of South America. *Journal of Vertebrate Paleontology* 2: 362–371.
- Brochu, C.A. 1996. Closure of neurocentral sutures during crocodylian ontogeny: implications for maturity assessment in fossil archosaurs. *Journal of Vertebrate Paleontology* 16: 49–62.
- Brusatte, S.L., Benton, M.J., Desojo, J.B., and Langer, M.C. 2010. The higher-level phylogeny of Archosauria (Tetrapoda: Diapsida). *Journal of Systematic Palaeontology* 8: 3–47.
- Butler, R.J., Nesbitt, S.J., Charig, A.J., Gower, D.J., and Barrett, P.M. 2018. *Mandasuchus tanyauchen*, gen. et sp. nov., a pseudosuchian archosaur from the Manda Beds (?Middle Triassic) of Tanzania. *Journal of Vertebrate Paleontology* 37: 96–121.
- Butler, R.J., Sullivan, C., Ezcurra, M.D., Liu, J., Lecuona, A., and Sookias, R.B. 2014. New clade of enigmatic early archosaurs yields insights into early pseudosuchian phylogeny and the biogeography of the archosaur radiation. *BMC Evolutionary Biology* 14: 128.
- Casamiquela, R.M. 1960. Noticia preliminar sobre dos nuevos estagonolepoides argentinos. *Ameghiniana* 2: 3–9.
- Clark, J.M., Sues, H.D., and Berman, D.S. 2001. A new specimen of *Hesperosuchus agilis* from the Upper Triassic of New Mexico and the interrelationships of basal crocodylomorph archosaurs. *Journal of Vertebrate Paleontology* 20: 683–704.
- Colbert, E.H. 1952. A pseudosuchian reptile from Arizona. *Bulletin of the American Museum of Natural History* 99: 561–592.
- Colbert, E.H. 1989. The Triassic dinosaur *Coelophysis*. *Bulletin of the Museum of Northern Arizona* 57: 1–174.
- Colbert, E.H. and Mook, C.C. 1951. The ancestral crocodylian *Protosuchus*. *Bulletin of the American Museum of Natural History* 97: 143–182.
- Colombi, C.E. 2007. *Historia tafonómica de las comunidades fósiles de la Formación Ischigualasto (Triásico Superior, Carniano), San Juan, Argentina*. 290 pp. Unpublished Ph.D. Dissertation, Universidad Nacional de San Juan, San Juan.
- Colombi, C.E. and Parrish, J.T. 2008. Late Triassic environmental evolution in southwestern Pangea: Plant taphonomy of the Ischigualasto Formation. *Palaios* 23: 778–795.
- Colombi, C.E., Rogers, R.R., and Alcober, O.A. 2012. Vertebrate taphonomy of the Ischigualasto Formation. *Journal of Vertebrate Paleontology* 32: 31–50.
- Cope, E.D. 1869. Synopsis of the extinct Batrachia, Reptilia and Aves of North America. *Transactions of the American Philosophical Society* 14: 1–252.
- Crush, P.J. 1984. A late Upper Triassic sphenosuchid crocodylian from Wales. *Palaentology* 27: 131–157.
- Currie, B.S., Colombi, C.E., Tabor, N.J., Shipman, T.C., and Montañez, I.P. 2009. Stratigraphy and architecture of the Upper Triassic Ischigualasto Formation, Ischigualasto Provincial Park, San Juan, Argentina. *Journal of South American Earth Sciences* 27: 74–87.
- Desojo, J.B. 2005. *Los aetosaurios (Amniota, Diapsida) de América del Sur: sus relaciones y aportes a la biogeografía y bioestratigrafía del Triásico continental*. 175 pp. Unpublished Ph.D. Thesis, Universidad de Buenos Aires, Buenos Aires.
- Desojo, J.B. and Ezcurra, M.D. 2011. A reappraisal of the taxonomic status of *Aetosauroides* (Archosauria, Aetosauria) specimens from the Late Triassic of South America and their proposed synonymy with *Stagonolepis*. *Journal of Vertebrate Paleontology* 31: 596–609.
- Desojo, J.B., Fiorelli, L.E., Ezcurra, M.D., Martinelli, A.G., Ramezani, J., Da Rosa, Á.A.S., Baczko, M.B. von, Trotteyn, M.J., Montefeltro, F.C., Ezpeleta, M., and Langer, M.C. 2020. The Late Triassic Ischigualasto Formation at Cerro Las Lajas (La Rioja, Argentina): fossil tetrapods, high-resolution chronostratigraphy, and faunal correlations. *Scientific Reports* 10: 1–34.
- Dzik, J. 2003. A beaked herbivorous archosaur with dinosaur affinities from the early Late Triassic of Poland. *Journal of Vertebrate Paleontology* 23: 556–574.
- Ezcurra, M.D. and Butler, R.J. 2018. The rise of the ruling reptiles and ecosystem recovery from the Permo-Triassic mass extinction. *Proceedings of the Royal Society B: Biological Sciences* 285: 20180361.
- Foth, C., Ezcurra, M.D., Sookias, R.B., Brusatte, S.L., and Butler, R.J. 2016. Unappreciated diversification of stem archosaurs during the Middle Triassic predated the dominance of dinosaurs. *BMC Evolutionary Biology* 16: 188.
- Galton, P.M. 1978. Fabrosauridae, the basal family of ornithischian dinosaurs (Reptilia: Ornithopoda). *Paläontologische Zeitschrift* 52: 138–159.
- Galton, P.M. 2000. Are *Spondylosoma* and *Staurikosaurus* (Santa Maria Formation, Middle–Upper Triassic, Brazil) the oldest saurischian dinosaurs? *Paläontologische Zeitschrift* 74: 393–423.
- Gauthier, J.A. 1984. *A Cladistic Analysis of the Higher Categories of the Diapsida*. 564 pp. Ph.D. Thesis, University of California, Berkeley.
- Gauthier, J. and Padian, K. 1985. Phylogenetic, functional, and aerodynamic analyses of the origin of birds and their flight. In: J.H.O.M.K. Hecht, G. Viohl, and P. Wellnhofer (eds.), *The Beginning of Birds*, 185–197. Freunde des Jura Museums, Eichstatt.
- Gauthier, J.A., Kluge, A.G., and Rowe, T. 1988. Amniote phylogeny and the importance of fossils. *Cladistics* 4: 105–209.
- Goloboff, P.A. and Catalano, S.A. 2016. TNT version 1.5, including a full implementation of phylogenetic morphometrics. *Cladistics* 32: 221–238.
- Goloboff, P.A., Farris, J.S., and Nixon, K.C. 2008. TNT, a free program for phylogenetic analysis. *Cladistics* 24: 774–786.
- Goloboff, P.A., Farris, J.S., Källersjö, M., Oxelman, B., Ramirez, M.J., and Szumik, C.A. 2003. Improvements to resampling measures of group support. *Cladistics* 19: 324–332.
- Gower, D.J. and Schoch, R.R. 2009. Postcranial anatomy of the rauisuchian archosaur *Batrachotomus kupferzellensis*. *Journal of Vertebrate Paleontology* 29: 103–122.
- Hoffman, D.K., Edwards, H.R., Barrett, P.M., and Nesbitt, S.J. 2019. Reconstructing the archosaur radiation using a Middle Triassic archosauriform tooth assemblage from Tanzania. *PeerJ* 7: e7970.
- Hoffstetter, R. and Gasc, J.P. 1969. Vertebrae and ribs of modern reptiles. In: C. Gans (ed.), *Biology of the Reptilia. Volume 1*, 201–210. Academic Press, New York.
- Huene, F. von 1942. *Die fossilen Reptilien des südamerikanischen Gondwanalandes, Ergebnisse der Sauriergrabungen in Südbrasilien 1928/29*. 332 pp. C.H. Becksche, München.
- Hyder, E.S., Witton, M.P., and Martill, D.M. 2014. Evolution of the pterosaur pelvis. *Acta Palaeontologica Polonica* 59: 109–125.

- Irmis, R.B. 2007. Axial skeleton ontogeny in the Parasuchia (Archosauria: Pseudosuchia) and its implications for ontogenetic determination in archosaurs. *Journal of Vertebrate Paleontology* 27: 350–361.
- Irmis, R.B., Nesbitt, S.J., and Sues, H.D. 2013. Early crocodylomorpha. *Geological Society, London, Special Publications* 379: 275–302.
- Irmis, R.B., Nesbitt, S.J., Padian, K., Smith, N.D., Turner, A.H., Woody, D., and Downs, A. 2007. A Late Triassic dinosauro-morph assemblage from New Mexico and the rise of dinosaurs. *Science* 317: 358–361.
- Kambic, R.E., Biewener, A.A., and Pierce, S.E. 2017. Experimental determination of three-dimensional cervical joint mobility in the avian neck. *Frontiers in Zoology* 14: 1–15.
- Kearney, M. and Clark, J.M. 2003. Problems due to missing data in phylogenetic analyses including fossils: a critical review. *Journal of Vertebrate Paleontology* 23: 263–274.
- Kent, D.V., Malnis, P.S., Colombi, C.E., Alcober, O.A., and Martínez, R.N. 2014. Age constraints on the dispersal of dinosaurs in the Late Triassic from magnetostratigraphy of the Los Colorados Formation (Argentina). *Proceedings of the National Academy of Sciences* 111: 7958–7963.
- Krebs, B. 1965. Die Triasfauna der Tessiner Kalkalpen. XIX. *Ticinosuchus ferox*, nov. gen. nov. sp. Ein neuer Pseudosuchier aus der Trias des Monte San Giorgio. *Schweizerische Palaontologische Abhandlungen* 81: 1–140.
- Laurin, M. 1991. The osteology of a Lower Permian eosuchian from Texas and a review of diapsid phylogeny. *Zoological Journal of the Linnean Society* 101: 59–95.
- Lautenschlager, S. and Desojo, J.B. 2011. Reassessment of the Middle Triassic rauisuchian archosaurs *Ticinosuchus ferox* and *Stagonosuchus nyassicus*. *Palaontologische Zeitschrift* 85: 357–381.
- Lautenschlager, S. and Rauhut, O.W. 2015. Osteology of *Rauisuchus tiradentes* from the Late Triassic (Carnian) Santa Maria Formation of Brazil, and its implications for rauisuchid anatomy and phylogeny. *Zoological Journal of the Linnean Society* 173: 55–91.
- Leardi, J.M., Pol, D., and Clark, J.M. 2017. Detailed anatomy of the braincase of *Macelognathus vagans* Marsh, 1884 (Archosauria, Crocodylomorpha) using high resolution tomography and new insights on basal crocodylomorph phylogeny. *PeerJ* 5: e2801.
- Leardi, J.M., Pol, D., Novas, F.E., and Suárez Riglos, M. 2015. The postcranial anatomy of *Yacarerani boliviensis* and the phylogenetic significance of the notosuchian postcranial skeleton. *Journal of Vertebrate Paleontology* 35: e995187.
- Leardi, J.M., Yáñez, I., and Pol, D. 2020. South American Crocodylomorphs (Archosauria; Crocodylomorpha): A review of the early fossil record in the continent and its relevance on understanding the origins of the clade. *Journal of South American Earth Sciences* [published online, <https://doi.org/10.1016/j.jsames.2020.102780>].
- Lecuona, A. 2013. *Anatomía y relaciones filogenéticas de Gracilisuchus stipanicorum y sus implicancias en el origen de Crocodylomorpha*. 145 pp. Unpublished Ph.D. Thesis, Universidad de Buenos Aires, Buenos Aires.
- Lecuona, A. and Desojo, J.B. 2012. Hind limb osteology of *Gracilisuchus stipanicorum* (Archosauria: Pseudosuchia). *Earth and Environmental Science Transactions of the Royal Society of Edinburgh* 102: 105–128.
- Lecuona, A., Desojo, J.B., and Pol, D. 2017. New information on the postcranial skeleton of *Gracilisuchus stipanicorum* (Archosauria: Suchia) and reappraisal of its phylogenetic position. *Zoological Journal of the Linnean Society* 181: 638–677.
- Lecuona, A., Ezcurra, M.D., and Irmis, R.B. 2016. Revision of the early crocodylomorph *Trialetes romeri* (Archosauria, Suchia) from the lower Upper Triassic Ischigualasto Formation of Argentina: one of the oldest-known crocodylomorphs. *Papers in Palaeontology* 2: 585–622.
- Li, C., Wu, X.C., Cheng, Y.N., Sato, T., and Wang, L. 2006. An unusual archosaurian from the marine Triassic of China. *Naturwissenschaften* 93: 200–206.
- Liparini, A. and Schultz, C.L. 2013. A reconstruction of the thigh musculature of the extinct pseudosuchian *Prestosuchus chiniquensis* from the *Dinodontosaurus* Assemblage Zone (Middle Triassic epoch), Santa Maria 1 Sequence, southern Brazil. *Geological Society, London, Special Publications* 379: 441–468.
- López-Gamundi, O.R., Espejo, I.S., Conaghan, P.J., and Powell, C.McA. 1994. Southern South America. In: J.J. Veivers and C.McA. Powell (eds.), *Permian–Triassic Pangean Basins and Foldbelts Along the Panthalassan Margin of Gondwanaland*. *Geological Society of America, Memoir* 184: 281–329.
- Mancuso, A.C., Gaetano, L.C., Leardi, J.M., Abdala, F., and Arcucci, A.B. 2014. The Chañares Formation: a window to a Middle Triassic tetrapod community. *Lethaia* 47: 244–265.
- Marsicano, C.A., Irmis, R.B., Mancuso, A.C., Mundil, R., and Chemale, F. 2016. The precise temporal calibration of dinosaur origins. *Proceedings of the National Academy of Sciences* 113: 509–513.
- Martínez, R.N. 1994. *Estratigrafía del Sector Agua de la Peña–Río de la Chilca, Formación Ischigualasto (Triásico Superior), Cuenca de Ischigualasto, San Juan*. 90 pp. Unpublished M.Sc. Thesis, Universidad Nacional de San Juan, San Juan.
- Martínez, R.N., Apaldetti, C., Alcober, O.A., Colombi, C.E., Sereno, P.C., Fernández, E., Santi Malnis, P., Correa, G.A., and Abelin, D. 2012. Vertebrate succession in the Ischigualasto Formation. *Journal of Vertebrate Paleontology* 32: 10–30.
- Martínez, R.N., Sereno, P.C., Alcober, O.A., Colombi, C.E., Renne, P.R., Montañez, I.P., and Currie, B.S. 2011. A basal dinosaur from the dawn of the dinosaur era in southwestern Pangaea. *Science* 331: 206–210.
- Mastrantonio, B.M. 2010. *Descrição Osteológica de Materiais Cranianos e Pós-cranianos de Prestosuchus chiniquensis (Archosauria, Rauisuchia) do Mesotriássico do RS (Biosfera de Dinodontosaurus, Formação Santa Maria) e Considerações Filogenéticas sobre Rauisúquios*. 244 pp. Ph.D. Thesis, Programa de Pós-Graduação em Geociências, Universidade Federal do Rio Grande do Sul, Porto Alegre.
- Milana, J.P. and Alcober, O. 1994. Modelo tectosedimentario de la cuenca triásica de Ischigualasto (San Juan, Argentina). *Revista de la Asociación Geológica Argentina* 49: 217–235.
- Molnar, J.L., Pierce, S.E., and Hutchinson, J.R. 2014. An experimental and morphometric test of the relationship between vertebral morphology and joint stiffness in Nile crocodiles (*Crocodylus niloticus*). *Journal of Experimental Biology* 217: 758–768.
- Mook, C.C. 1921. Notes on the postcranial skeleton in the Crocodilia. *Bulletin of the American Museum of Natural History* 44: 67–100.
- Nesbitt, S.J. 2005. Osteology of the Middle Triassic pseudosuchian archosaur *Arizonasaurus babbitti*. *Historical Biology* 17: 19–47.
- Nesbitt, S. 2007. The anatomy of *Effigia okeeffeae* (Archosauria, Suchia), theropod-like convergence, and the distribution of related taxa. *Bulletin of the American Museum of Natural History* 302: 1–84.
- Nesbitt, S.J. 2011. The early evolution of archosaurs: relationships and the origin of major clades. *Bulletin of the American Museum of Natural History* 352: 1–292.
- Nesbitt, S.J. and Butler, R.J. 2013. Redescription of the archosaur *Par-ringtonia gracilis* from the Middle Triassic Manda Beds of Tanzania, and the antiquity of Erpetosuchidae. *Geological Magazine* 150: 225–238.
- Nesbitt, S.J., Butler, R.J., Ezcurra, M.D., Barrett, P.M., Stocker, M.R., Angielczyk, K.D., Smith, R.M.H., Sidor, C.A., Niedzwiedzki, G., Sen-nikov, A., and Charig, A.J. 2017. The earliest bird-line archosaurs and the assembly of the dinosaur body plan. *Nature* 544: 484–487.
- Nesbitt, S.J., Butler, R.J., Ezcurra, M.D., Charig, A.J., and Barrett, P.M. 2018. The anatomy of *Teleocrater rhadinus*, an early avemetatarsalian from the lower portion of the Lifua Member of the Manda Beds (Middle Triassic). *Journal of Vertebrate Paleontology* 37: 142–177.
- Nesbitt, S.J., Irmis, R.B., Parker, W.G., Smith, N.D., Turner, A.H., and Rowe, T. 2009. Hindlimb osteology and distribution of basal dinosauro-morphs from the Late Triassic of North America. *Journal of Vertebrate Paleontology* 29: 498–516.
- Nesbitt, S., Liu, J., and Li, C. 2010a. A sail-backed suchian from the Heshanggou Formation (Early Triassic: Olenekian) of China. *Earth and Environmental Science Transactions of the Royal Society of Edinburgh* 101: 271–284.

- Nesbitt, S.J., Sidor, C.A., Angielczyk, K.D., Smith, R.M., and Tsuji, L.A. 2014. A new archosaur from the Manda Beds (Anisian, Middle Triassic) of southern Tanzania and its implications for character state optimizations at Archosauria and Pseudosuchia. *Journal of Vertebrate Paleontology* 34: 1357–1382.
- Nesbitt, S.J., Sidor, C.A., Irmis, R.B., Angielczyk, K.D., Smith, R.M., and Tsuji, L. A. 2010b. Ecologically distinct dinosaurian sister group shows early diversification of Ornithodira. *Nature* 464: 95–98.
- Organ, C.L. 2006. Thoracic epaxial muscles in living archosaurs and ornithomimid dinosaurs. *Anatomical Records* 288: 782–793.
- Osborn, H.F. 1903. The reptilian subclasses Diapsida and Synapsida and the early history of the Diaptosauria. *Memoirs of the Museum of Natural History* 1 (8): 449–519.
- Parker, W.G. and Nesbitt, S.J. 2013. Cranial remains of *Poposaurus gracilis* (Pseudosuchia: Popsauroida) from the Upper Triassic, the distribution of the taxon, and its implications for popsauroid evolution. *Geological Society, London, Special Publications* 379: 503–523.
- Parrish, J.M. 1993. Phylogeny of the Crocodylotarsi, with reference to archosaurian and crurotarsan monophyly. *Journal of Vertebrate Paleontology* 13: 287–308.
- Peyer, K., Carter, J.G., Sues, H.D., Novak, S.E., and Olsen, P.E. 2008. A new suchian archosaur from the Upper Triassic of North Carolina. *Journal of Vertebrate Paleontology* 28: 363–381.
- Pol, D. and Escapa, I.H. 2009. Unstable taxa in cladistic analysis: identification and the assessment of relevant characters. *Cladistics* 25: 515–527.
- Pol, D., Leardi, J.M., Lecuona, A., and Krause, M. 2012. Postcranial anatomy of *Sebecus icaeorhinus* (Crocodyliformes, Sebecidae) from the Eocene of Patagonia. *Journal of Vertebrate Paleontology* 32: 328–354.
- Ramos, V.A. and Kay, S.M. 1991. Triassic rifting and associated basalts in the Cuyo Basin, central Argentina. In: R.S. Harmon and C.W. Rapela (eds.), *Andean Magmatism and its Tectonic Setting*. *Geological Society of America Special Paper* 265: 79–91.
- Reig, O.A. 1963. La presencia de dinosaurios saurisquios en los “Estratos de Ischigualasto”, (Mesotriásico superior) de las provincias de San Juan y La Rioja (República Argentina). *Ameghiniana* 3: 3–20.
- Rogers, R.R., Arcucci, A.B., Abdala, F., Sereno, P.C., Forster, C.A., and May, C.L. 2001. Paleoenvironment and taphonomy of the Chañares Formation tetrapod assemblage (Middle Triassic), northwestern Argentina: spectacular preservation in volcanogenic concretions. *Palaos* 16: 461–481.
- Rogers, R.R., Swisher, C.C., Sereno, P.C., Monetta, A.M., Forster, C.A., and Martínez, R.N. 1993. The Ischigualasto tetrapod assemblage (Late Triassic, Argentina) and $^{40}\text{Ar}/^{39}\text{Ar}$ dating of dinosaur origins. *Science* 260: 794–797.
- Romer, A.S. 1972. The Chañares (Argentina) Triassic reptile fauna. XIV. *Lewisuchus admixtus*, gen. et sp. nov., a further thecodont from the Chañares Beds. *Breviora* 390: 1–13.
- Sen, K. 2005. A new rauisuchian archosaur from the Middle Triassic of India. *Palaontology* 48: 185–196.
- Sereno, P.C. and Arcucci, A.B. 1994a. Dinosaurian precursors from the Middle Triassic of Argentina: *Lagerpeton chanarensis*. *Journal of Vertebrate Paleontology* 13: 385–399.
- Sereno, P.C. and Arcucci, A.B. 1994b. Dinosaurian precursors from the Middle Triassic of Argentina: *Marasuchus lilloensis*, gen. nov. *Journal of Vertebrate Paleontology* 14: 53–73.
- Sereno, P.C., Forster, C.A., Rogers, R.R., and Monetta, A.M. 1993. Primitive dinosaur skeleton from Argentina and the early evolution of Dinosauria. *Nature* 361: 64–66.
- Sereno, P.C., Martínez, R.N., and Alcober, O.A. 2012. Osteology of *Eoraptor lunensis* (Dinosauria, Sauropodomorpha). *Journal of Vertebrate Paleontology* 32: 83–179.
- Schachner, E.R., Manning, P.L., and Dodson, P. 2011. Pelvic and hindlimb myology of the basal archosaur *Poposaurus gracilis* (Archosauria: Popsauroida). *Journal of Morphology* 272: 1464–1491.
- Sill, W.D. 1974. The anatomy of *Saurosuchus galilei* and the relationships of the rauisuchid thecodonts. *Bulletin of the Museum of Comparative Zoology* 146: 317–362.
- Sues, H.D., Olsen, P.E., Carter, J.G., and Scott, D.M. 2003. A new crocodylomorph archosaur from the Upper Triassic of North Carolina. *Journal of Vertebrate Paleontology* 23: 329–343.
- Sulej, T. 2005. A new rauisuchian reptile (Diapsida: Archosauria) from the Late Triassic of Poland. *Journal of Vertebrate Paleontology* 25: 78–86.
- Tabor, N.J., Montañez, I.P., Kelso, K.A., Currie, B., Shipman, T., and Colombi, C. 2006. A Late Triassic soil catena: landscape and climate controls on paleosol morphology and chemistry across the Carnian-age Ischigualasto–Villa Union Basin, northwestern Argentina. *Geological Society of America Bulletin, Special Paper* 416: 17–41.
- Trottey, M.J., Desojo, J.B., and Alcober, O.A. 2011. Nuevo material postcraneano de *Saurosuchus galilei* Reig (Archosauria: Crurotarsi) del Triásico Superior del centro-oeste de Argentina. *Ameghiniana* 48: 13–28.
- Tsuihiji, T. 2004. The ligament system in the neck of *Rhea americana* and its implication for the bifurcated neural spines of sauropod dinosaurs. *Journal of Vertebrate Paleontology* 24: 165–172.
- Tsuihiji, T. 2005. Homologies of the transversospinalis muscles in the anterior presacral region of Sauria (crown Diapsida). *Journal of Morphology* 263: 151–178.
- Uliana, M.A. and K.T. Biddle. 1988. Mesozoic–Cenozoic paleogeographic and geodynamic evolution of southern South America. *Revista Brasileira de Geociências* 18: 172–190.
- Walker, A.D. 1990. A revision of *Sphenosuchus acutus* Haughton, crocodylomorph reptile from the Elliot Formation (Late Triassic or Early Jurassic) of South Africa. *Philosophical Transactions of the Royal Society of London B Biological Sciences* 330: 1–120.
- Weinbaum, J.C. and Hungerbühler, A. 2007. A revision of *Poposaurus gracilis* (Archosauria: Suchia) based on two new specimens from the Late Triassic of the southwestern USA. *Paläontologische Zeitschrift* 81: 131–145.
- Weinbaum, J.C. 2013. Postcranial skeleton of *Postosuchus kirkpatricki* (Archosauria: Paracrocodylomorpha), from the Upper Triassic of the United States. *Geological Society, London, Special Publications* 379: 525–553.
- Wellnhofer, P. 2003. A Late Triassic pterosaur from the Northern Calcareous Alps (Tyrol, Austria). *Geological Society, London, Special Publications* 217: 5–22.
- Wilson, J.A. 1999. A nomenclature for vertebral laminae in sauropods and other saurischian dinosaurs. *Journal of Vertebrate Paleontology* 19: 639–653.
- Wu, X.C. 1981. The discovery of a new thecodont from north east Shanxi. *Vertebrata Palasiatica* 19: 122–132.
- Wu, X.C. and Chatterjee, S. 1993. *Dibothrosuchus elaphros*, a crocodylomorph from the Lower Jurassic of China and the phylogeny of the Sphenosuchia. *Journal of Vertebrate Paleontology* 13: 58–89.
- Wu, X.C. and Russell, A.P. 2001. Redescription of *Turfanosuchus dabanensis* (Archosauriformes) and new information on its phylogenetic relationships. *Journal of Vertebrate Paleontology* 21: 40–50.

Appendix 1

List of taxa used for comparisons

Alligator mississippiensis (Mook 1921)
Arizonasaurus babbitt (Nesbitt 2005)
Asilisaurus kongwe (Nesbitt et al. 2010b)
Batrachotomus kupferzellensis (Gower and Schoch 2009)
 CM 73372 (Nesbitt et al. 2011; Weinbaum 2013; JML photographs)
Coelophysis bauri (Colbert 1989)
Dibothrosuchus elaphros (Wu and Chatterjee 1993)
Dimorphodon macronyx (Hyder et al. 2014)
Dongusuchus efremovi (Niedźwiedzki et al. 2014)
Dromicosuchus grallator (Sues et al. 2003)
Dromomeron gregorii (Nesbitt et al. 2009)
Dromomeron romeri (Irmis et al. 2007)
Effigia okeeffeae (Nesbitt 2007)
Eodromeus murphi (Martínez et al. 2011)
Eoraptor lunensis (Sereno et al. 1993, 2012)
Erpetosuchus granti (Benton and Walker 2002)
Eudimorphodon ranzii (Wellnhofer 2003)
Fasolasuchus tenax (Bonaparte 1981)
Gracilisuchus stipanicorum (Lecuona and Desojo 2011; Lecuona 2013; Lecuona et al. 2017)
Hesperosuchus agilis AMNH 6758 (Colbert 1952)
Hesperosuchus agilis UCM 12947 (Parrish 1993)
Lagerpeton chanarensis (Sereno and Arcucci 1994a)
Lesothosaurus diagnosticus (Galton 1978)
Lewisuchus admixtus (Romer 1972; Bittencourt et al. 2015)
Mandasuchus tanyauchen (Butler et al. 2018)
Marasuchus lilloensis (Sereno and Arcucci 1994b)
Nundasuchus songeaensis (Nesbitt et al. 2014)
Parringtonia gracilis (Nesbitt and Butler 2013)
Polonosuchus silesiacus (Sulej 2005)
Poposaurus gracilis (Weinbaum and Hungerbühler 2007; Parker and Nesbitt 2013)
Poposaurus gracilis TTU-P 10419 (Weinbaum and Hungerbühler 2007)
Postosuchus alisonae (Peyer et al. 2008)
Postosuchus kirkpatricki TTU-P 9235 (Weinbaum 2013)
Prestosuchus chiniquensis UFRGS-PV-0629-T (Mastrantonio 2010; Liparini and Schultz 2013)
Protosuchus richardsoni (Colbert and Mook 1951)
Pseudhesperosuchus jachaleri (Bonaparte 1971)
Qianosuchus mixtus (Li et al. 2006; Nesbitt 2011)
Rauisuchus tiradentes (Lautenschlager and Desojo 2015)
Riojasuchus tenuiceps (Bonaparte 1971; Baczko and Ezcurra 2013)
Saurosuchus galilei (Sill 1974; Trotteyn et al. 2011)
Silesaurus opolensis (Dzik 2003)
Sillosuchus longicervix (Alcober and Parrish 1997)
Sphenosuchus acutus (Walker 1990)
Spondylosoma absconditum (Huene 1942; Galton 2000)
Teleocrater rhadinus (Nesbitt et al. 2017; Nesbitt et al. 2018)
Terrestriusuchus gracilis (Crush 1984)
Ticinosuchus ferox (Krebs 1965; Lautenschlager and Desojo 2011)
Trialestes romeri (Bonaparte 1997; Lecuona et al. 2016)
Tropidosuchus romeri (Arcucci 1990)
Turfanosuchus dabanensis (Wu and Russel 2001)
Xilousuchus sapingensis (Wu 1981; Nesbitt et al. 2010a)
Yarasuchus deccanensis (Sen 2005)